

Ni⁰-Catalyzed Cyclotrimerization of 1,3-Butadiene: A Comprehensive Density Functional Investigation on the Origin of the Selectivity

Sven Tobisch*^[a]

Abstract: A comprehensive theoretical investigation of the mechanism for the Ni⁰-catalyzed cyclotrimerization of 1,3-butadiene by the [Ni⁰(η^2 -butadiene)₃] active catalyst complex is presented by employing a gradient-corrected DFT method. All critical elementary processes of the catalytic cycle have been scrutinized, namely, oxidative coupling of two butadienes, butadiene insertion into the allyl–Ni^{II} bond, allylic isomerization in both octadienediyl–Ni^{II} and dodecatrienediyl–Ni^{II} species, and reductive elimination under ring closure. For each of these elementary steps several conceivable routes and also the different stereochemical pathways have been probed. The favorable route for oxidative coupling start from the prevalent [Ni⁰(η^2 -butadiene)₃] form of the

active catalyst through coupling between the terminal non-coordinated carbon atoms of two reactive η^2 -butadiene moieties; this is assisted by an ancillary butadiene in η^2 -mode. The initial $\eta^3, \eta^1(\text{C}^1)$ -octadienediyl–Ni^{II} product is the active precursor for subsequent butadiene insertion, which preferably takes place into the η^3 -allyl–Ni^{II} bond. The insertion is driven by a strong thermodynamic force. Therefore, the dodecatrienediyl–Ni^{II} products, with the most favorable bis(η^3 -allyl) Δ -*trans* isomers in particular, represent a ther-

modynamic sink. Commencing from a preestablished equilibrium between the various bis(η^3 -allyl) Δ -*trans* forms of the [Ni^{II}(dodecatrienediyl)] complex, the major cyclotrimer products, namely all-*t*-CDT, *c,c,t*-CDT and *c,t,t*-CDT, are formed along competing paths by reductive elimination under ring closure, which is shown to be rate-controlling. The all-*c*-CDT-generating path is completely precluded by both thermodynamic and kinetic factors, giving rise to negligibly populated bis(η^3 -allyl) Δ -*cis* precursor isomers. The regulation of the selectivity of the CDT formation as well as the competition between the two reaction channels for generation of C₁₂- and C₈-cycloolefins is elucidated.

Keywords: density functional calculations • dienes • nickel • reaction mechanisms • structure-reactivity relationships

Introduction

The catalytic cyclotrimerization of 1,3-dienes mediated by transition-metal complexes is one of the key reactions in homogeneous catalysis.^[1] Several transition-metal complexes and Ziegler–Natta catalyst systems have been established that actively catalyze the stereoselective cyclotrimerization of 1,3-dienes.^[2] Nickel complexes, in particular, have been demonstrated to be the most versatile catalysts.^[3] The cyclotrimerization is not only confined to 1,3-butadiene; substituted butadienes, and 1,3,5-hexatriene are also known to react.^[1a, 4]

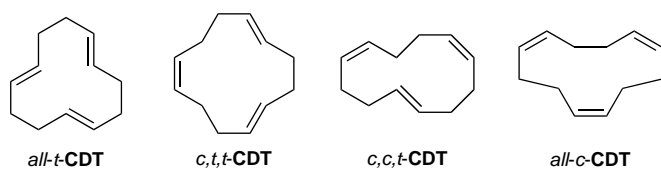
The catalytic cyclotrimerization of 1,3-butadiene to 1,5,9-cyclododecatriene (CDT) was first reported by Reed who used modified Reppe catalysts.^[5] It was Wilke, however, who discovered the first practical synthesis of CDT with typical Ziegler–Natta catalysts.^[2a] In further comprehensive and systematic investigations Wilke and co-workers provided a detailed insight into the Ni⁰-catalyzed cyclotrimerization of 1,3-butadiene.^[3, 6] The isolation and characterization of a bis(η^3)-dodecatrienediyl–Ni^{II} complex as a reactive intermediate^[7] and the examination of individual elementary steps by stoichiometric reactions demonstrated important cornerstones in the development of mechanistic understanding of homogenous catalysis.

The zerovalent [Ni⁰(butadiene)_x] complex is the active catalyst, and can be formed, for example, by reducing a nickel salt in the presence of butadiene^[8] or alternatively by using a zerovalent “bare” nickel complex by ligand displacement with butadiene. Three of the four possible isomers of CDT, namely all-*t*-CDT, *c,c,t*-CDT, and *c,t,t*-CDT, are formed in the Ni⁰-catalyzed cyclotrimerization. All-*t*-CDT is the predominant product (over 90% selectivity), while all-*c*-CDT is not formed.^[9]

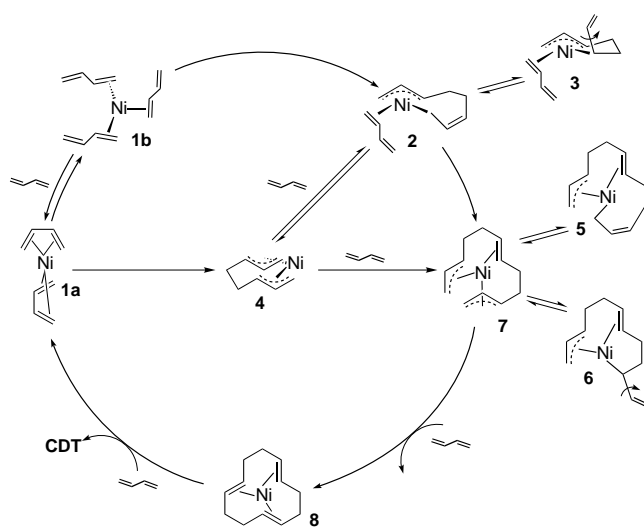
[a] Dr. S. Tobisch

Institut für Anorganische Chemie
der Martin-Luther-Universität Halle-Wittenberg
Fachbereich Chemie, Kurt-Mothes-Strasse 2
06210 Halle (Germany)
Fax: (+49) 345-5527028
E-mail: tobisch@chemie.uni-halle.de

Supporting information for this article is available on the WWW under <http://www.wiley-vch.de/home/chemistry> or from the author.



The Ni^0 -catalyzed cyclotrimerization of butadiene has unequivocally been shown to occur in a multistep fashion. The nickel atom template undergoes a repeated change in its formal oxidation state, namely, $[\text{Ni}^0 \rightleftharpoons \text{Ni}^{\text{II}}]$, during the multistep addition–elimination mechanism. The general catalytic cycle proposed by Wilke et al. is shown in Scheme 1.^[3] The



Scheme 1. Catalytic cycle of the Ni^0 -catalyzed cyclotrimerization of 1,3-butadiene.

$[\text{Ni}^0(\text{butadiene})_x]$ complex represents the active catalyst complex, which can exist in several forms of either $[\text{Ni}^0(\text{butadiene})_2]$ **1a** or the $[\text{Ni}^0(\text{butadiene})_3]$ **1b** species. Oxidative coupling of two butadienes gives rise to the octadienediyl– Ni^{II} complex, which may be coordinatively saturated by complexation of butadiene. This complex occurs in several configurations, which are distinguished by the different coordination of the octadienediyl framework, namely, the η^3, η^1 species **2** and **3**, and the bis(η^3) species **4**, all of which are in equilibrium. Butadiene insertion into the allyl– Ni^{II} bond in either of the octadienediyl– Ni^{II} species leads to the $[\text{Ni}^{\text{II}}(\text{dodecatrienediyl})]$ complex. Similar to the octadienediyl– Ni^{II} species, the dodecatrienediyl– Ni^{II} species are present in the η^3, η^1 configurations **5** and **6**, and the bis(η^3) configuration **7** as well. The $[\text{Ni}^0(\text{CDT})]$ product complex **8**, which may be stabilized by coordination of an additional butadiene, is formed by reductive elimination under ring closure starting from the $[\text{Ni}^{\text{II}}(\text{dodecatrienediyl})]$ complex. The formation of the various isomers of CDT occurs through competing pathways for reductive elimination that involve different stereoisomers. Displacement of the cyclotrimer product in subsequent consecutive substitution steps with butadiene, which is supposed to take place without a significant barrier,

regenerates the $[\text{Ni}^0(\text{butadiene})_x]$ active catalyst, thereby completing the catalytic cycle.

Most of the individual steps of the proposed catalytic cycle have precedence in the chemistry of organonickel compounds and have been decisively supported by the stoichiometric cyclotrimerization reaction. Although the $[\text{Ni}^0(\text{butadiene})_x]$ active catalyst has never been experimentally characterized, formal $16e^-$ or $18e^-$ forms of species **1a** and **1b**, respectively, are likely candidates. A $[\text{Ni}^0(\eta^4\text{-cis-2,3-dimethylbutadiene})_2]$ complex, with the two *cis*-butadienes coordinated in a tetrahedral manner, is well known^[10, 11] and has been shown to yield an $\eta^3, \eta^1(\text{C}^1)$ -octadienediyl– Ni^{II} complex in the reaction with donor phosphines (e.g., PCy_3).^[10] The various configurations of octadienediyl– Ni^{II} compounds have been firmly established for $\text{PR}_3/\text{P}(\text{OR})_3$ -stabilized species by both NMR spectroscopy and by X-ray structural analysis.^[10, 12] The rearrangement between the different configurations is shown to be facile.^[12a] The bis(η^1) species of octadienediyl– Ni^{II} and dodecatrienediyl– Ni^{II} complexes, although conceivable as reactive intermediates for allylic isomerization and/or reductive elimination, are not likely to play any role within the catalytic cycle.^[13] The $[\text{Ni}^{\text{II}}(\text{bis}(\eta^3), \Delta\text{-dodecatrienediyl})]$ intermediate has been isolated in the stoichiometric reaction of zerovalent nickel complexes with butadiene at -40°C .^[7, 9a] An NMR spectroscopic investigation has confirmed two stereoisomers, which are energetically close, for the isolated $[\text{Ni}^{\text{II}}(\text{bis}(\eta^3\text{-anti}), \Delta\text{-trans-dodecatrienediyl})]$ intermediate. These isomers are distinguished by opposite enantiofaces of the coordinated olefinic double bond.^[11, 14] The reaction of the dodecatrienediyl– Ni^{II} intermediate with PMe_3 at low temperature was followed by NMR spectroscopy and revealed a facile allylic isomerization prior to reductive elimination; this occurs only at elevated temperatures and gives rise to a mixture of *all-t*-CDT and *c,t,t*-CDT.^[15] Reductive elimination along a direct path (i.e., without prior isomerization), which would give *c,c,t*-CDT, is indicated to be kinetically impeded, as a consequence of the *trans* orientation of terminal carbon of the two *anti*-allylic groups. For reductive elimination along feasible pathways one or both allylic groups have to undergo prior isomerization, thus leading to *c,t,t*-CDT and *all-t*-CDT, respectively. Starting from the dodecatrienediyl– Ni^{II} complex, it has been demonstrated that the formation of the twelve-membered ring in stoichiometric reactions is facilitated by the presence of donor phosphines (i.e., PMe_3 , PET_3 , PPh_3) and also by excess butadiene.^[9a, 16] The formal $16e^-$ $[\text{Ni}^0(\text{CDT})]$ product, a well-established zerovalent nickel complex (in particular the *all-t*-CDT isomer),^[17] is known to form stable adducts with donor ligands.^[1a, 3b, 10, 18]

It is the objective of the present computational study to extend the mechanistic insight into the Ni^0 -catalyzed cyclotrimerization of 1,3-butadiene by clarifying the following intriguing, but still not firmly resolved aspects:

- 1) What is the thermodynamically most stable form of the $[\text{Ni}^0(\text{butadiene})_x]$ catalyst complex, and which of the various forms is the catalytically active species?
- 2) Which form of the octadienediyl– Ni^{II} complex is initially formed by oxidative coupling, and which of the different species, namely **2**, **3**, or **4**, represent the precursor for butadiene insertion into the allyl– Ni^{II} bond?

- 3) Is the isolated $[\text{Ni}^{\text{II}}(\text{bis}(\eta^3\text{-anti}), \Delta\text{-trans-dodecatrienediyl})]$ intermediate directly involved in the course of the catalytic cyclotrimerization?
- 4) Which of the crucial elementary steps is rate-determining?
- 5) What are the critical factors that control the stereo-selective generation of only three of the possible four stereoisomers of CDT, and what are the reasons leading to the all-*t*-CDT isomer being predominantly formed?

All critical elementary reaction processes occurring along different conceivable routes have been scrutinized, taking into account oxidative coupling of two butadiene moieties, butadiene insertion into the allyl–Ni^{II} bond, allylic isomerization, and reductive elimination under ring closure. The present study is to the best of our knowledge, the first comprehensive theoretical mechanistic investigation of the complete catalytic cycle for the catalytic cyclotrimerization of 1,3-butadiene mediated by zerovalent “bare” nickel complexes. This represents a further part of our systematic theoretical exploration of crucial structure–reactivity relationships in transition-metal-assisted cyclooligomerization reactions of 1,3-dienes. In previous investigations we have scrutinized the C₈-cycloolefin generation reaction channel of the nickel-catalyzed cyclooligomerization of 1,3-butadiene for a generic catalyst,^[19a] and have also been able to elucidate the influence of electronic and steric factors for all critical elementary processes as well as for the regulation of the product selectivity for real catalysts.^[19b]

Computational Details

All reported DFT calculations were performed by employing the program package TURBOMOLE developed by Häser and Ahlrichs.^[20] The calculations were carried out by using the LDA with Slater's exchange functional^[21a,b] and Vosko–Wilk–Nusair parameterization on the homogeneous electron gas for correlation,^[21c] augmented with gradient-corrected functionals for electron exchange according to Becke^[21d] and correlation according to Perdew^[21e,f] in a self-consistent fashion. This gradient-corrected density functional is usually termed BP86 in the literature. In recent benchmark computational studies, it was shown that the BP86 functional gives results in excellent agreement with the best wave function-based method available today, for the class of reactions investigated here.^[22]

For all atoms a standard all-electron basis set of triple- ζ quality for the valence electrons augmented with polarization functions was employed for the geometry optimization and the saddle-point search. The Wachters 14s/9p/5d set^[23a] supplemented by two diffuse p^[23a] and one diffuse d function^[23b] contracted to (62111111/5111111/3111) was used for nickel, and standard TZVP basis sets^[23c] were used for phosphorous (a 13s/9p/1d set contracted to (73111/6111/1)), carbon (a 10s/6p/1d set contracted to (7111/411/1)), and hydrogen (a 5s/1p set contracted to (311/1)). The frequency calculations were done by using standard DZVP basis sets,^[23c] which consist of a 15s/9p/5d set contracted to (63321/531/41) for nickel, a 12s/8p/1d set contracted to (6321/521/1) for phosphorous, a 9s/5p/1d set contracted to (621/41/1) for carbon, and a 5s set contracted to (41) for hydrogen, for DZVP optimized structures, which differ in marginal extent from the triple- ζ optimized ones. The corresponding auxiliary basis sets were used for fitting the charge density.^[23c,d] This is the standard computational methodology utilized throughout this paper.

The geometry optimization and the saddle-point search were carried out at the BP86 level of approximation by utilizing analytical/numerical gradients/Hessians according to standard algorithms. No symmetry constraints were imposed in any case. The stationary points were identified exactly by the curvature of the potential-energy surface at these points corresponding to the eigenvalues of the Hessian. The various forms and stereoisomers of

1–8 (cf. Scheme 1) were exactly identified as minima, while all reported transition states have exactly one negative Hessian eigenvalue. The reaction and activation enthalpies and free energies (ΔH , ΔH^\ddagger and ΔG , ΔG^\ddagger at 298 K and 1 atm) were calculated for the most stable isomers of each of the key species of the entire catalytic reaction. The reactant and product that correspond directly to the located transition-state structure were checked by following the reaction pathway going downhill to both sides from slightly relaxed transition-state structures.

Results and Discussion

First, each of the elementary processes in Scheme 1 will be explored step-by-step followed by discussion of the factors that are decisive for the regulation of the selectivity of the CDT formation. The various possible stereochemical pathways, which originate from the enantioface and the configuration (*s-trans* or *s-cis*) of the prochiral butadiene moieties involved, have been carefully examined for each of the elementary steps. The individual stereochemical pathways are denoted by a pictorial representation of the participating butadiene's configurations and enantiofaces.^[24] The discussion below is concentrated on the most feasible of the various stereochemical pathways for each of the elementary steps. The complete collection of energetic data for all possible stereochemical pathways is available as Supporting Information (Tables S1–S6).

A) Oxidative coupling of two coordinated butadienes: The active catalyst $[\text{Ni}^0(\text{butadiene})_x]$ complex can exist in several forms, with $[\text{Ni}^0(\text{butadiene})_2]$ (**1a**) and $[\text{Ni}^0(\text{butadiene})_3]$ (**1b**) being the most probable, since they bear resemblance to the known $[\text{Ni}^0(\eta^4\text{-cis-1,3-dimethylbutadiene})_2]$ ^[10, 11] and $[\text{Ni}^0(\text{ethylene})_3]$ ^[25] complexes. Bis(η^4)-butadiene and η^4, η^2 -butadiene, and tris(η^2)-butadiene and $\eta^4, \text{bis}(\eta^2)$ -butadiene forms are conceivable for **1a** and **1b**, respectively, depending on whether butadiene coordinates in monodentate (η^2) or bidentate (η^4) fashion. Several isomers for each of these forms have been located. The relative thermodynamic stability of the most favorable isomers for each of these forms is reported in Table 1. For the formal 18e⁻ quasi tetrahedral bis(η^4) and $\eta^4, \text{bis}(\eta^2)$ forms, the η^4 -butadiene preferably

Table 1. Thermodynamic stability [$\Delta H/\Delta G$ in kcalmol⁻¹] of the most favorable isomers of $[\text{Ni}^0(\text{butadiene})_2]$ (**1a**) and $[\text{Ni}^0(\text{butadiene})_3]$ (**1b**) of the active catalyst complex.^[a,b]

1a	1a	1b	1b
bis($\eta^4\text{-cis}$)	$\eta^4\text{-trans}, \eta^2\text{-trans}$	tris($\eta^2\text{-trans}$)	$\eta^4\text{-cis}, \text{bis}(\eta^2\text{-trans})$
6.3/–4.3	6.9/–5.2	0.0/0.0	3.3/4.3

[a] Numbers in italics are the Gibbs free energies. [b] The complete collection of all isomers is included in the Supporting Information (Table S1).

coordinates in $\eta^4\text{-cis}$ mode, while for the formal 16e⁻ η^4, η^2 -butadiene forms the $\eta^4\text{-trans}$ mode is favored. For butadiene to coordinate monodentate, the $\eta^2\text{-trans}$ mode prevails over the $\eta^2\text{-cis}$ mode for all forms.

The formal 16e⁻ trigonal planar tris(η^2)-butadiene form of the $[\text{Ni}^0(\text{butadiene})_3]$ species **1b**, with the tris($\eta^2\text{-trans}$) isomer most favorable, are predicted to be thermodynamically

preferred at the enthalpy surface (ΔH). The $[\text{Ni}^0(\text{butadiene})_2]$ species **1a**, with the most stable bis(η^4 -*cis*)-butadiene and η^4 -*trans*, η^2 -*trans* forms found to be close in energy, are $\sim 6.6 \text{ kcal mol}^{-1}$ higher in enthalpy. By taking the gas-phase-calculated entropic contributions into account, the $[\text{Ni}^0(\text{butadiene})_2]$ species **1a** should be the predominant compound at the free-energy surface (ΔG). However, the calculated gas-phase entropies are not suitable to allow a balanced description of butadiene association and dissociation processes under the actual catalytic reaction conditions.^[9b, 26] It has to be concluded that the $[\text{Ni}^0(\eta^2\text{-butadiene})_3]$ species **1b** is the prevailing compound of the active catalyst at actual catalytic conditions. The order of the calculated stability for tris(η^2)-butadiene isomers reflects the preference for the η^2 -*trans* over the η^2 -*cis* coordination. On the other hand, isomers arising from butadiene coordinating with different enantiofaces are close in energy (cf. Table S1 in the Supporting Information).

The oxidative coupling was examined for several paths with the different forms of the catalyst complex acting as possible precursors. Two feasible routes for oxidative coupling of two coordinated butadiene moieties have been found. The first route is characterized by a transition-state structure with the formation of the new C–C σ -bond between the terminal non-coordinated carbon (C^4 , C^5) of two reactive η^2 -butadiene moieties (Figure 1) assisted by an ancillary butadiene in η^2 -mode. Commencing from the tris(η^2)-butadiene form of **1b** and crossing the transition state, the $[\text{Ni}^{\text{II}}(\eta^3, \eta^1(\text{C}^1), \Delta\text{-octadienediyl})(\eta^2\text{-butadiene})]$ species **2** is formed as the initial coupling product. With the different isomers of the η^4 , bis(η^2)-butadiene form of **1b** acting as precursor, the systems always approach the corresponding tris(η^2)-butadiene isomers in the vicinity of the transition state. Thus, the path with tris(η^2)-butadiene transition states is energetically preferred for all forms of **1b** along the **1b** \rightarrow **2** route. The second route, which

involves the bis(η^4)-butadiene form (Figure 2) proceeds via a transition state for formation of the new C–C σ -bond between

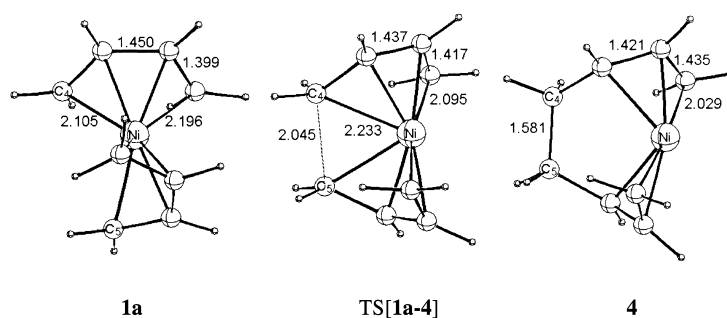


Figure 2. Selected geometric parameters [\AA] of the optimized structures of key species for oxidative coupling by the most feasible pathway for η^4 -*cis*/ η^4 -*cis*-butadiene coupling along the **1a** \rightarrow **4** route commencing from the $[\text{Ni}^0(\eta^4\text{-butadiene})_2]$ precursor **1a**.

two η^4 -butadienes, affording the $[\text{Ni}^{\text{II}}(\text{bis}(\eta^3)\text{-octadienediyl})]$ species **4** as the kinetic coupling product. The **1a** \rightarrow **4** route with the bis(η^4)-butadiene form is favorable for all isomers of **1a**, since the same kind of transition state was located when starting from η^4, η^2 -butadiene precursors.

The energetics of the oxidative coupling along **1b** \rightarrow **2** are collected in Table 2 for different stereochemical pathways, and the key species involved along the most feasible pathway are given in Figure 1. The transition state for C–C bond formation between the two uncoordinated terminal carbons (C^4 , C^5) of the two η^2 -butadiene moieties, TS[**1b-2**], appears reactant-like and occurs at a distance of ~ 2.20 – 2.30 \AA for the emerging C–C σ -bond. The kinetic barrier as well as the thermodynamic driving force for oxidative coupling is mainly determined by the configuration and the enantioface of the two reactive butadiene moieties involved in the process, while the ancillary butadiene has a minor influence.^[27] Very similar intrinsic barriers arise for identical coupling stereoisomers with the auxiliary butadiene in either *s-cis* or *s-trans* configuration (cf. Table S2 in the Supporting Information). In terms of total barriers, however, an ancillary *trans*-butadiene favors the oxidative coupling by ~ 2 – 3 kcal mol^{-1} , relative to *cis*-butadiene counterparts, due to both kinetic and thermodynamic reasons. This reflects the thermodynamic prevalence of

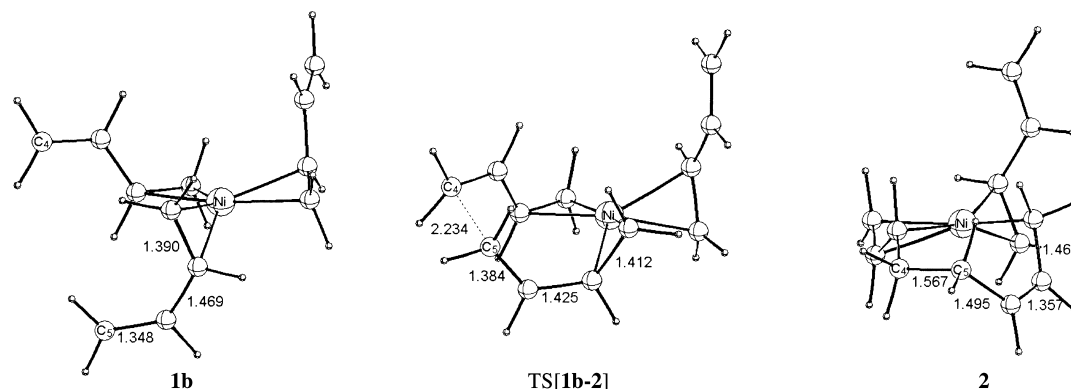


Figure 1. Selected geometric parameters [\AA] of the optimized structures of key species for oxidative coupling by the most feasible pathway for η^2 -*trans*/ η^2 -*cis*-butadiene coupling (of opposite enantiofaces) along the **1b** \rightarrow **2** route commencing from the $[\text{Ni}^0(\eta^2\text{-butadiene})_3]$ precursor **1b**.

Table 2. Activation enthalpies and free energies [$\Delta H^\ddagger/\Delta G^\ddagger$ in kcal mol⁻¹] and reaction enthalpies and free energies [$\Delta H/\Delta G$ in kcal mol⁻¹] for oxidative coupling of two η^2 -butadienes along **1b** → **2**, with the [Ni⁰(η^2 -butadiene)₃] species **1b** as precursor.^[a–f]

Isomer of 2 Coupling isomer ^[24]	1b	TS[1b-2]	2
η^3 -anti, η^1 (C ¹), Δ -cis 	5.6/5.0	14.8/16.8	-1.2/1.8
	6.0/5.1	25.0/26.5	2.4/5.1
η^3 -syn, η^1 (C ¹), Δ -cis 	3.3/2.9	18.2/19.8	-0.7/2.1
	2.9/2.6	10.5/12.6	-3.1/-0.4
η^3 -syn, η^1 (C ¹), Δ -trans 	0.0/0.0	12.9/14.9	10.0/12.1
	0.4/0.4	15.9/17.7	13.4/15.5

[a] This process is classified according to the butadiene coupling stereoisomers (indicated by its pictorial representation)^[24] involved. The relationship between the butadiene coupling isomers and the stereoisomers of **2** is explicitly given. [b] Total barriers and reaction energies relative to the most stable isomer of the [Ni⁰(η^2 -butadiene)₃] active catalyst species **1b**; namely [Ni⁰(η^2 -trans-butadiene)₃]. [c] Numbers in italics are the Gibbs free energies. [d] The lowest barrier of the individual stereochemical pathways is in boldface type. [e] The enantioface of the ancillary butadiene involved does negligible influence the energetics of the process, as indicated by () () . [f] Only the stereochemical pathways with an ancillary η^2 -trans-butadiene are reported; the complete collection is included in the Supporting Information (Table S2).

the η^2 -trans mode. Further discussions will focus on these isomers.

The kinetic η^3, η^1 (C¹) coupling product **2** is formed in an overall thermoneutral process, except for the coupling of two η^2 -trans-butadienes, which affords strained products. The most feasible stereochemical pathway proceeds by the coupling of η^2 -trans/ η^2 -cis-butadienes of opposite enantiofaces with a free-energy barrier of 12.6 kcal mol⁻¹ (ΔG^\ddagger), giving rise to the most stable [Ni^{II}(η^3 -syn, η^1 (C¹), Δ -cis)-octadienediyl](η^2 -trans-butadiene) isomer of **2**. Hence, this pathway is favored owing to both kinetic and thermodynamic reasons. It is interesting to note that the same η^3, η^1 -octadienediyl–Ni^{II} stereoisomer has been unequivocally established as the initial coupling product for the PR₃/P(OR)₃-stabilized [Ni⁰(butadiene)₂L] complex, which catalyzes the formation of C₈-cycloolefins.^[10, 12] The coupling of two η^2 -trans and two η^2 -cis butadienes preferably occurs with the two moieties having identical enantiofaces, with barriers that are 2.3 and 4.2 kcal mol⁻¹ (ΔG^\ddagger) larger than the kinetically preferred η^2 -trans/ η^2 -cis coupling.

The coupling of two η^4 -butadienes along **1a** → **4** proceeds via the product-like transition state TS[**1a-4**] (Figure 2), which is characterized by a nearly complete pre-formation of the two allylic moieties. The thermodynamically most favorable bis(η^4 -cis) isomer is also seen to be kinetically preferred by the overall lowest barrier of 25.0 kcal mol⁻¹ (ΔH^\ddagger relative to **1b**, cf. Table 3), while the coupling of two η^4 -trans butadiene moieties is impeded by large barriers. The transition state for the coupling of two trans-butadienes with opposite enantiofaces could not be located; this might occur at significantly higher energy.

Identical stereochemical pathways are seen to be kinetically preferred along **1b** → **2** and **1a** → **4** for coupling of *cis/cis*-

Table 3. Activation enthalpies and free energies [$\Delta H^\ddagger/\Delta G^\ddagger$ in kcal mol⁻¹] and reaction enthalpies and free energies [$\Delta H/\Delta G$ in kcal mol⁻¹] for oxidative coupling of two η^4 -butadienes along **1a** → **4**, with the [Ni⁰(η^4 -butadiene)₂] species **1a** as precursor.^[a–d]

Isomer of 4 Coupling isomer ^[24]	1a	TS[1a-4]	4
bis(η^3 -anti) 	6.3/–4.3	25.0/16.2	10.1/1.3
	6.3/–4.3	32.1/23.2	3.3/–6.0
η^3 -syn/ η^3 -anti 	12.7/0.9	52.4/42.9	5.5/–3.5
	12.7/0.9	38.8/29.4	
bis(η^3 -syn) 	13.6/2.1	61.5/51.7	1.0/–8.0
	13.6/2.1		4.3/–5.2

[a] This process is classified according to the butadiene coupling stereoisomers (indicated by its pictorial representation)^[24] involved. The relationship between the butadiene coupling isomers and the stereoisomers of **4** is explicitly given. [b] Total barriers and reaction energies relative to the most stable isomer of the [Ni⁰(η^2 -butadiene)₃] active catalyst species **1b**; namely [Ni⁰(η^2 -trans-butadiene)₃]. [c] Numbers in italics are the Gibbs free energies. [d] The lowest barrier of the individual stereochemical pathways is in boldface type.

trans/cis-, and *trans/trans*-butadiene. Comparison of the barriers connected with the most feasible pathways along the alternative routes demonstrates that oxidative coupling preferably takes place along **1b** → **2**. The **1a** → **4** route, however, is not feasible owing to an enthalpic barrier that is 14.5 kcal mol⁻¹ ($\Delta\Delta H^\ddagger$) larger.

The following conclusions can be drawn for the oxidative coupling elementary step. Tris(η^2 -)butadiene isomers of **1b** are shown to be predominant species of the active catalyst complex under catalytic reaction conditions^[9b, 26] and also represent the catalytically active species for oxidative coupling of two butadiene moieties. The coupling preferably takes place between η^2 -trans/ η^2 -cis-butadiene of opposite enantiofaces affording the η^3 -syn, η^1 (C¹), Δ -cis isomer of **2** owing to both kinetic and thermodynamic reasons.

B) Allylic isomerization in octadienediyl–Ni^{II} species: The various configurations of the octadienediyl–Ni^{II} coupling product, that is, the η^3, η^1 species **2**, **3**, and the bis(η^3) species **4**, are likely to readily undergo mutual conversion for identical stereoisomers. The conversion between stereoisomeric forms of the octadienediyl–Ni^{II} complex takes place through isomerization of one or both terminal allylic groups. The isomerization of the allylic group involves two aspects, first the interconversion of its *syn* and *anti* configuration and second the inversion of its enantioface.^[28] If oxidative coupling and subsequent butadiene insertion steps taking place along different stereochemical pathways, allylic isomerization may represent an indispensable step in the course of the catalytic process.

Allylic isomerization has been demonstrated to preferably proceed by an η^3 - π → η^1 - σ -C³ allylic rearrangement followed by internal rotation of the vinyl group around the formal C²–C³ single bond (Figure 3), both by experimental^[28, 29] and by theoretical^[30] evidence. Several stereochemical pathways have been investigated, with η^3 -syn, η^1 (C³) and η^3 -anti, η^1 (C³) isomers of the [Ni^{II}(η^3, η^1 (C³)-octadienediyl)(η^2 -butadiene)]

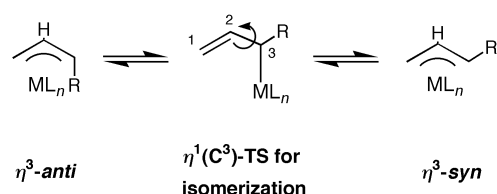


Figure 3. Allylic isomerization taking place via an $\eta^1(\text{C}^3)$ -allylic intermediate.

compound **3** acting as precursor and to occur through formal $16e^-$ rotational transition states $\text{TS}_{\text{ISO}}[\mathbf{3}]$, which corresponds to the internal vinyl group's rotation around the $\text{C}^2\text{--C}^3$ bond (Figure 4). Furthermore, it has been probed explicitly whether additional butadiene could assist this process.

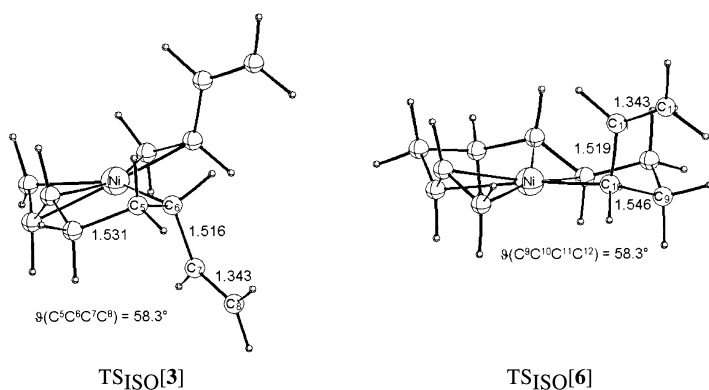


Figure 4. Selected geometric parameters [\AA] of the optimized rotational transition-state structures for allylic isomerization via the $\eta^3\text{-syn}, \eta^1(\text{C}^3)$ -octadienediyl- Ni^{II} $\text{TS}_{\text{ISO}}[\mathbf{3}]$ ($\eta^3\text{-syn}, \eta^1(\text{C}^3)\text{-syn}$ (syn-syn) \rightleftharpoons $\eta^3\text{-syn}, \eta^1(\text{C}^3)\text{-anti}$ (syn-anti)) process, Table 4) and the $\eta^3\text{-syn}, \eta^1(\text{C}^3), \Delta\text{-trans}$ -dodecatrienediyl- Ni^{II} $\text{TS}_{\text{ISO}}[\mathbf{6}]$ ($\eta^3\text{-syn}, \eta^1(\text{C}^3)\text{-syn}, \Delta\text{-trans}$ ($\text{syn-syn}, \Delta\text{-trans}$) \rightleftharpoons $\eta^3\text{-syn}, \eta^1(\text{C}^3)\text{-anti}, \Delta\text{-trans}$ ($\text{syn-anti}, \Delta\text{-trans}$)) process, Table 6), respectively.

Similar to the findings in the previous section, an ancillary $\eta^2\text{-trans}$ -butadiene lowers the total isomerization barrier by ~ 2 kcal mol $^{-1}$ (ΔG^\ddagger , cf. Table S3 in the Supporting Information) compared to *cis*-butadiene congeners, while the auxiliary butadiene's enantioface involved has a negligible influence on the energetics. From the total free-energies of activation via $\text{TS}_{\text{ISO}}[\mathbf{3}]$ collected in Table 4 it is quite evident that allylic isomerization involving $\eta^3\text{-syn}, \eta^1(\text{C}^3)$ isomers (i.e., conversion between $\eta^2\text{-trans}/\eta^2\text{-cis}$ -butadiene and $\eta^2\text{-trans}/\eta^2\text{-trans}$ -butadiene coupling products) is a facile process with a barrier of 8.6–9.4 kcal mol $^{-1}$ (ΔG^\ddagger relative to the favorable isomer of **2**), while isomerization commencing from corresponding $\eta^3\text{-anti}, \eta^1(\text{C}^3)$ isomers (i.e., conversion between $\eta^2\text{-trans}/\eta^2\text{-cis}$ -butadiene and $\eta^2\text{-cis}/\eta^2\text{-cis}$ -butadiene coupling products) is predicted to be significantly slower as a result of associated barriers, which are approximately as twice as large (16.0–18.0 kcal mol $^{-1}$, ΔG^\ddagger). Thermodynamic reasons are seen to be critical for the different total reactivities of the $\eta^3\text{-syn}, \eta^1(\text{C}^3)$ and the $\eta^3\text{-anti}, \eta^1(\text{C}^3)$ isomers to undergo allylic isomerization. Both forms show similar intrinsic reactivities, as indicated by similar intrinsic barriers of ~ 7.1 kcal mol $^{-1}$ ($\Delta G_{\text{int}}^\ddagger$, relative to the corresponding stereoisomer of the precursor **3**). However, $\eta^3\text{-anti}, \eta^1(\text{C}^3)$ isomers of **3** are

Table 4. Activation enthalpies and free energies [$\Delta H^\ddagger/\Delta G^\ddagger$ in kcal mol $^{-1}$] for allylic isomerization via $\text{TS}_{\text{ISO}}[\mathbf{3}]$ with the $[\text{Ni}^{\text{II}}(\eta^3, \eta^1(\text{C}^3)\text{-octadienediyl})(\eta^2\text{-butadiene})]$ species **3** as precursor.^[a–f]

Isomer of 3 Coupling isomer ^[24]	Isomer of 3 Coupling isomer ^[24]	$\text{TS}_{\text{ISO}}[\mathbf{3}]$
$\eta^3\text{-anti}, \eta^1(\text{C}^3)\text{-syn} \rightarrow$ 	$\eta^3\text{-anti}, \eta^1(\text{C}^3)\text{-anti}$ 	15.8/16.0
$\eta^3\text{-syn}, \eta^1(\text{C}^3)\text{-syn} \rightarrow$ 	$\eta^3\text{-syn}, \eta^1(\text{C}^3)\text{-anti}$ 	18.2/18.0
$\eta^3\text{-syn}, \eta^1(\text{C}^3)\text{-syn} \rightarrow$ 	$\eta^3\text{-syn}, \eta^1(\text{C}^3)\text{-syn}$ 	9.2/9.4
$\eta^3\text{-syn}, \eta^1(\text{C}^3)\text{-syn} \rightarrow$ 	$\eta^3\text{-syn}, \eta^1(\text{C}^3)\text{-syn}$ 	8.1/8.6

[a] This process is classified according to the butadiene coupling stereoisomers (indicated by its pictorial representation)^[24] involved. The relationship between the butadiene coupling isomers and the stereoisomers of **3** is explicitly given. [b] Total barriers relative to the most stable isomer of **2**; namely $[\text{Ni}^{\text{II}}(\eta^3\text{-syn}, \eta^1(\text{C}^1), \Delta\text{-cis}\text{-octadienediyl})(\eta^2\text{-trans}\text{-butadiene})]$. [c] Numbers in italics are the Gibbs free energies. [d] The lowest barrier of the individual stereochemical pathways is in boldface type. [e] The enantioface of the ancillary butadiene involved does negligible influence the energetics of the process, as indicated by (syn-syn). [f] Only the stereochemical pathways with an ancillary $\eta^2\text{-trans}$ -butadiene are reported; the complete collection is included in the Supporting Information (Table S3).

thermodynamically disfavored by more than 7.4 kcal mol $^{-1}$ (ΔG) relative to the $\eta^3\text{-syn}, \eta^1(\text{C}^3)$ counterparts. The $\eta^3\text{-syn}, \eta^1(\text{C}^3)$ and $\eta^3\text{-anti}, \eta^1(\text{C}^3)$ isomers are connected by a facile $\eta^3\text{-syn}, \eta^1\text{-anti} \rightleftharpoons \eta^3\text{-anti}, \eta^1\text{-syn}$ conversion. This intramolecular $\eta^3/\eta^1 \rightleftharpoons \eta^1/\eta^3$ shift should proceed readily, since linear transit calculations give no indication for the existence of a notable barrier.

Several isomers of $\text{TS}_{\text{ISO}}[\mathbf{3}]\text{-BD}$ with a further $\eta^2\text{-trans}$ -butadiene attached have been located. All of these isomers are characterized by two weakly bound butadiene moieties, which are ~ 9 kcal mol $^{-1}$ (ΔH) above the separated species $\{\text{TS}_{\text{ISO}}[\mathbf{3}] + \text{trans-butadiene}\}$. Therefore, it must be concluded, that incoming butadiene does not serve to accelerate allylic isomerization through the stabilization of $\text{TS}_{\text{ISO}}[\mathbf{3}]$ and, hence, additional butadiene is not likely to participate in this process.

C) Butadiene insertion into the allyl- Ni^{II} bond of octadienediyl- Ni^{II} species: Commencing from the octadienediyl- Ni^{II} oxidative coupling product, butadiene insertion into the allyl- Ni^{II} bond can occur along several routes, most of which have been examined. In general, the most favorable transition states along the different routes are characterized by a quasi-planar arrangement of the reacting moieties; namely the terminal carbon of the allylic group, the nickel atom, and the coordinated butadiene's double bond that will be inserted. With the $\eta^3, \eta^1(\text{C}^1)$ species **2** acting as precursor, butadiene can be inserted into either the η^3 - or the $\eta^1(\text{C}^1)$ -allyl- Ni^{II} bond. Square-planar (SP) transition-state structures, in which η^2 -butadiene resides in a square-planar conformation together with the η^3 - and $\eta^1(\text{C}^1)$ -allylic groups have been located. Along with them, transition-state structures of square-pyramidal (SPY) and trigonal-bipyramidal (TBP) configuration for η^4 -butadiene insertion into the η^3 - and $\eta^1(\text{C}^1)$ -allyl- Ni^{II} bond, respectively, have also been located. The η^1 -allylic group, which is preferably situated in equatorial positions, is shifted to an axial position in SPY and TBP transition states, caused by bidentate monomer coordination. Only $\eta^4\text{-cis}$ -butadiene is seen to have a notable tendency to

compete for coordination with the $\eta^1(\text{C}^1)$ -allylic group, while for η^4 -*trans*-butadiene SPY and TBP transition-state structures could not be located. Starting from different initial structures, the η^4 -*trans*-butadiene species always relax into the corresponding SP transition-state structure. For all stereochemical pathways, the transition state for η^4 -butadiene insertion lies at least 3.3 kcal mol⁻¹ above that for η^2 -butadiene insertion. Thus, an SP transition state for η^2 -butadiene insertion is most likely to be encountered along the route starting from **2**.

For the alternative insertion route commencing from $\eta^3, \eta^1(\text{C}^3)$ species **3**, SP and TBP transition states are involved along possible pathways for η^2 - and η^4 -butadiene insertion into the η^3 -allyl–Ni^{II} bond, respectively, that bear great resemblance to those discussed for $\eta^3, \eta^1(\text{C}^1)$ species **2**. Similar to the findings in the last paragraph, butadiene insertion preferably takes place via an SP transition state.

As a further alternative, an insertion route has been probed that involves bis(η^3) species **4**. Commencing from several isomers of SPY [Ni^{II}(bis(η^3)-octadienediyl)(η^2 -butadiene)] species **4-BD**, in which butadiene adopts the axial position, and following the reaction pathway in a linear transit approach,^[31] a facile $\eta^3 \rightarrow \eta^1(\text{C}^1)$ allylic rearrangement is revealed in the vicinity of the transition state. Thus, the systems always lead to the SP transition-state structure discussed above that corresponds to the η^2 -butadiene insertion into the η^3 -allyl–Ni^{II} bond of $\eta^3, \eta^1(\text{C}^3)$ species **2**. The transition state structure directly connected to **4-BD**, which could not be located, is expected at higher energies. This leads to the conclusion, that bis(η^3) species **4-BD** are precluded from the energetically most favorable route for butadiene insertion, which is most likely to involve η^3, η^1 species.

Comparison of the barriers connected with the most feasible path (via SP transition states, cf. Table S4 in the Supporting Information) for η^2 -butadiene insertion into the allyl–Ni^{II} bond of $\eta^3, \eta^1(\text{C}^1)$ and $\eta^3, \eta^1(\text{C}^3)$ species, respectively, shows clearly that the route commencing from **2** is kinetically favored relative to the route that starts from **3** for all of the various stereochemical pathways, except for those with *trans/trans*-butadiene coupling products, in which lower barriers arise for $\eta^3, \eta^1(\text{C}^3)$ species. The preference of the alternative route via $\eta^3, \eta^1(\text{C}^3)$ species is, to a large part, attributed to the high steric strain associated with the η^3 -

syn, \eta^1(\text{C}^1), Δ -*trans* isomers; this makes these species unfavorable relative to the corresponding η^3 -*syn, \eta^1(\text{C}^3)*-*syn* species, in which the strain is less severe. It should be noted that *trans/trans*-butadiene coupling stereoisomers are not involved along feasible pathways for butadiene insertion (vide infra). Although they can be formed by facile allylic isomerization from the preferably generated η^3 -*syn, \eta^1(\text{C}^1)*, Δ -*cis* (*trans/cis*-butadiene coupling species) isomer of **2**, *trans/trans*-butadiene coupling stereoisomers should readily undergo the reverse **2** \rightarrow **1b** process, which is indicated to be significantly more facile than the **1b** \rightarrow **2** process. Thus, the *trans/trans*-butadiene coupling isomers of the octadienediyl–Ni^{II} complex should be negligibly populated. Accordingly, the corresponding insertion pathways have no relevance for the course of the catalytic process.

A further point of mechanistic interest concerns the question about which of the two allylic groups of the active $\eta^3, \eta^1(\text{C}^1)$ precursor **2** is more reactive in the process of butadiene insertion. For identical stereoisomers, the barriers for butadiene insertion into the η^3 -allyl–Ni^{II} bond are predicted to be always lower than the barrier of insertion into the $\eta^1(\text{C}^1)$ -allyl–Ni^{II} bond (cf. Table S4 in the Supporting Information). Therefore, butadiene is preferably inserted into the more reactive η^3 - π -allyl–Ni^{II} bond. A similar preference of the η^3 - π relative to the η^1 - σ coordination mode of the allyl–transition-metal bond has been demonstrated in theoretical investigations of the monomer insertion step in the allylnickel(II)-^[32a,b] and allyltitanium(II)-catalyzed^[32c] polymerization of 1,3-butadiene and also for the α -olefin insertion into the allyl–Zr^{III} bond.^[33]

The formation of the [Ni^{II}(dodecatrienediyl)] complex is shown to preferably take place by insertion of η^2 -butadiene into the η^3 -allyl–Ni^{II} bond of $\eta^3, \eta^1(\text{C}^1)$ -octadienediyl–Ni^{II} species **2** via the SP transition state TS[**2-7**]. Among the different configurations of the dodecatrienediyl–Ni^{II} insertion product complex, the [Ni^{II}(bis(η^3), Δ -dodecatrienediyl)] species **7** is thermodynamically favored. The key species involved in this process are displayed in Figure 5 for a representative case and the energetics of critical stereoisomeric pathways are collected in Table 5.

The most feasible of the various stereochemical pathways for insertion (cf. Table 5 and Table S4 in the Supporting Information) is seen to involve the *trans/cis*-butadiene coupling product **2** (i.e., the η^3 -*syn, \eta^1(\text{C}^1)*, Δ -*cis*-octadienediyl–

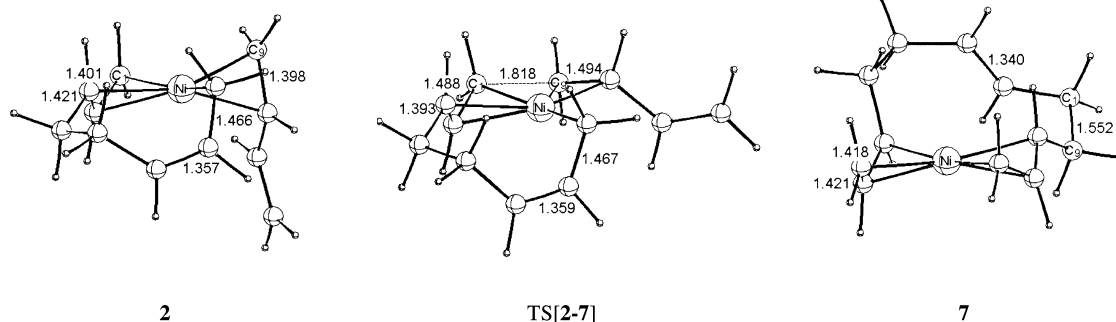


Figure 5. Selected geometric parameters [\AA] of the optimized structures of key species for butadiene insertion into the η^3 -allyl–Ni^{II} bond by the most feasible pathway (η^2 -*trans*-butadiene insertion into the η^3 -*syn*-allyl–Ni^{II} bond of *trans/cis*-butadiene coupling species **2** (indicated by the pictorial representation in Table 5) along **2** \rightarrow **7**.

Table 5. Activation enthalpies and free energies [$\Delta H^\ddagger/\Delta G^\ddagger$ in kcal mol⁻¹] and reaction enthalpies and free energies [$\Delta H/\Delta G$ in kcal mol⁻¹] for butadiene insertion into the η^3 -allyl–Ni^{II} bond along $\mathbf{2} \rightarrow \mathbf{7}$.^[a–e]

Butadiene insertion path ^[d] Coupling isomer ^[24]	2	TS[2 – 7]	7
<i>c</i> -BD into η^3 - <i>anti</i> -allyl 	η^3 - <i>anti</i> , η^1 (C ¹), Δ - <i>cis</i>		bis(η^3 - <i>anti</i>), Δ - <i>cis</i>
	4.4/4.3	20.4/21.7	–17.7/–14.7
	4.4/4.3	19.8/21.3	–6.9/–4.1
	8.2/8.1	22.7/23.8	–8.5/–6.6
	8.2/8.1	21.6/22.9	–11.4/–9.9
<i>t</i> -BD into η^3 - <i>anti</i> -allyl 	η^3 - <i>anti</i> , η^1 (C ¹), Δ - <i>cis</i>		η^3 - <i>anti</i> / η^3 - <i>syn</i> , Δ - <i>cis</i>
	1.9/2.2	19.7/21.2	–16.1/–14.3
	1.9/2.2	19.3/20.9	–15.6/–14.1
	5.5/5.5	20.2/21.7	–15.9/–14.2
	5.5/5.5	20.3/21.8	–15.6/–13.7
<i>c</i> -BD into η^3 - <i>syn</i> -allyl 	η^3 - <i>syn</i> , η^1 (C ¹), Δ - <i>cis</i>		bis(η^3 - <i>anti</i>), Δ - <i>trans</i>
	5.7/5.4	17.8/18.7	–17.0/–14.0
	5.7/5.4	16.4/17.5	–19.0/–15.8
	2.7/2.3	13.6/14.8	–17.0/–14.0
	2.7/2.3	14.1/15.1	–19.5/–16.4
<i>t</i> -BD into η^3 - <i>syn</i> -allyl 	η^3 - <i>syn</i> , η^1 (C ¹), Δ - <i>cis</i>		η^3 - <i>anti</i> / η^3 - <i>syn</i> , Δ - <i>trans</i>
	2.4/2.5	15.4/16.7	–12.8/–11.3
	2.4/2.5	15.7/16.8	–10.5/–9.5
	0.0/0.0	12.8/14.0	–15.5/–14.0
	0.0/0.0	13.1/14.4	–15.2/–13.6

[a] This process is classified according to the butadiene coupling stereoisomers (indicated by its pictorial representation)^[24] involved. The relation between the butadiene coupling, and the stereoisomers of **2** and **7** is explicitly given. [b] Total barriers and reaction energies relative to the most stable isomer of **2**; namely [Ni^{II}(η^3 -*syn*, η^1 (C¹), Δ -*cis*-octadienediyl)(η^2 -*trans*-butadiene)]. [c] Numbers in italics are the Gibbs free energies. [d] The lowest barrier of the individual stereochemical pathways is in boldface type. [e] Only few of the stereochemical pathways are reported; the complete collection is included in the Supporting Information (Table S4). [f] Butadiene insertion path; *c*-BD into η^3 -*anti*-allyl, denotes for example insertion of *cis*-butadiene into the η^3 -*anti*-allyl–Ni^{II} bond in **2**.

Ni^{II} isomer arising from opposite enantiofaces of the two butadiene moieties), which is formed under kinetic and thermodynamic control along $\mathbf{1b} \rightarrow \mathbf{2}$. Similar activation barriers of 14.0–15.1 kcal mol⁻¹ (ΔG^\ddagger) have to be overcome for insertion of *cis*- and *trans*-butadiene into the η^3 -*syn*–Ni^{II} bond, giving rise to bis(η^3 -*anti*), Δ -*trans* and η^3 -*syn*/ η^3 -*anti*, Δ -*trans* isomers of the dodecatrienediyl–Ni^{II} product species **7**, in a process that is highly exogonic by ~ -15 to -20 kcal mol⁻¹ (relative to the corresponding precursor isomer of **2**). On the other hand, butadiene insertion into either the η^3 -*anti*–Ni^{II} bond or the η^3 -*syn*–Ni^{II} bond of *cis*/*cis*-butadiene and *trans*/*trans*-butadiene coupling products, respectively, is less favorable due to corresponding transition states that are at distinct higher free energy ($\Delta\Delta G^\ddagger > 7$ kcal mol⁻¹).

To probe the possible participation of incoming monomer along $\mathbf{2} \rightarrow \mathbf{7}$, several [Ni^{II}(η^3 -*syn*, η^1 (C¹), Δ -*trans*-octadienediyl)(η^2 -*trans*-butadiene)₂] isomers for the precursor as well as for the transition state have been located. Similar to the findings for η^3 , η^1 (C³)-octadienediyl species (see Section B), these adducts with two loosely attached butadiene moieties are calculated to be at high energy. Thus additional butadiene does not serve to stabilize the precursor or the transition-state structure, either on the enthalpy surface or on the free-energy surface. Hence, incoming butadiene is not likely to assist the insertion process along $\mathbf{2} \rightarrow \mathbf{7}$.

To summarize, the following conclusions have to be drawn from the analysis of the oxidative coupling, allylic isomer-

ization, and insertion steps presented so far. The initially formed η^3 , η^1 (C¹) oxidative coupling product **2** represents also the catalytic active octadienediyl–Ni^{II} species for butadiene insertion. The η^3 -*syn*, η^1 (C¹), Δ -*cis* isomer (*trans*/*cis*-butadiene coupling product) is the predominant octadienediyl–Ni^{II} species that is preferably formed along $\mathbf{1b} \rightarrow \mathbf{2}$, due to both kinetic and thermodynamic reasons, with a barrier of 12.6 kcal mol⁻¹ (ΔG^\ddagger). The formation of *trans*/*trans*-butadiene and *cis*/*cis*-butadiene coupling products is less favorable, since these pathways are connected with free-energy barriers that are 2.3 and 4.2 kcal mol⁻¹ larger, respectively. Furthermore, the strained *trans*/*trans*-butadiene coupling products are also thermodynamically disfavored; thus their concentration might be very low as a result of a facile $\mathbf{2} \rightarrow \mathbf{1b}$ process. Conversion between *trans*/*cis*-butadiene and *trans*/*trans*-butadiene coupling isomers by η^3 -*syn*, η^1 (C³)-*anti* \rightleftharpoons η^3 -*syn*, η^1 (C³)-*syn* allylic isomerization is a facile process ($\Delta G^\ddagger = 8.6 - 9.4$ kcal mol⁻¹, Table 4), while the conversion between *trans*/*cis*-butadiene and *cis*/*cis*-butadiene coupling species (η^3 -*anti*, η^1 (C³)-*syn* \rightleftharpoons η^3 -*anti*, η^1 (C³)-*anti*) requires an activation energy (16.0–18.0 kcal mol⁻¹, ΔG^\ddagger , Table 4) that is larger than the barrier connected with the competitive butadiene insertion for *trans*/*cis*-butadiene coupling species (14.0–14.4 kcal mol⁻¹, ΔG^\ddagger , Table 5). Thus, *cis*/*cis*-butadiene coupling species **2** would not be present in appreciable concentrations. Furthermore, insertion along $\mathbf{2} \rightarrow \mathbf{7}$ by pathways that involves *cis*/*cis*-butadiene coupling species is kinetically impeded, since the associated barriers are distinct higher, relative to the most feasible pathway ($\Delta\Delta G^\ddagger > 7$ kcal mol⁻¹, Table 5). This leads to the conclusion, that the complete branch for generation of bis(allyl), Δ -*cis*-dodecatrienediyl–Ni^{II} forms is entirely suppressed first by the unfavorable coupling of two *cis*-butadienes along $\mathbf{1b} \rightarrow \mathbf{2}$ together with a slow isomerization via η^3 -*anti*, η^1 (C³) isomers of TS_{ISO}[**3**], giving rise to a low concentration of *cis*,*cis*-butadiene coupling η^3 -*anti*, η^1 (C¹), Δ -*cis* isomer of **2**, and second by the kinetically retarded butadiene insertion into the η^3 -*anti*-allyl–Ni^{II} bond along $\mathbf{2} \rightarrow \mathbf{7}$. Consequently, the path for generation of all-*c*-CDT, which would be accessible through formation of bis(η^3), Δ -*cis* isomers of **7**, followed by facile allylic isomerization (if required) and subsequent reductive elimination starting from bis(η^3 -*anti*), Δ -*cis*-dodecatrienediyl–Ni^{II} isomers, is entirely precluded. The most feasible pathway for oxidative coupling and insertion involves identical stereoisomers (*trans*/*cis*-butadiene coupling of opposite enantiofaces), Therefore, allylic isomerization in the octadienediyl–Ni^{II} complex is not required along the catalytic reaction course.

D) Allylic isomerization in dodecatrienediyl–Ni^{II} species:

Similar to octadienediyl–Ni^{II} complex, the η^3 , η^1 (C¹) (**5**), η^3 , η^1 (C¹) (**6**), and bis(η^3) (**7**) configurations of the [Ni^{II}(dodecatrienediyl)] product complex of insertion are also likely to undergo facile interconversion, with the bis(η^3) species **7** being thermodynamically most favorable. The generation of the [Ni^{II}(dodecatrienediyl)] complex along $\mathbf{2} \rightarrow \mathbf{7}$ represents the elementary process among all of the crucial elementary steps that is most exergonic. Therefore, **7** is likely to serve as a thermodynamic sink. This is supported by the isolation

of the bis(η^3 -*anti*), Δ -*trans* isomer of **7** as reactive intermediates in the stoichiometric cyclotrimerization.^[7, 9a]

Among the four possible stereoisomers for the isolated bis(η^3 -*anti*), Δ -*trans* intermediate, the two stereoisomers with *trans* oriented η^3 -*anti* allylic groups, which have been confirmed by NMR spectroscopy,^[11, 14] are predicted to be the thermodynamically most stable dodecatrienediyl–Ni^{II} species^[34] (Table 5, and Table S4 in the Supporting Information). The isolated bis(η^3 -*anti*), Δ -*trans* intermediates are formed along viable pathways for *cis*-butadiene insertion into the η^3 -*syn*–Ni^{II} bond of reactive *trans/cis*-butadiene coupling isomers of **2** (Table 5), and therefore are likely to be involved along the reaction course of the catalytic cyclotrimerization. In addition to the fact that the isolated intermediates are thermodynamically most favorable, the *trans* orientation of the two *anti*-allylic groups prevents facile reductive elimination due to connected insurmountable barriers (vide infra). This makes these stereoisomers of **7** ideal candidates for isolation at low temperatures, provided that allylic isomerization is connected with a significant barrier.

The discussion of the isomerization of the terminal allylic groups of the [Ni^{II}(dodecatrienediyl)] complex via η^3 , η^1 (C³) rotational transition states (TS_{ISO}[**6**]) is exclusively focused on bis(allyl), Δ -*trans* isomers, (Table 6, Figure 4). The corresponding bis(allyl), Δ -*cis* isomers are indicated to be negligibly

Table 6. Activation enthalpies and free energies [$\Delta H^\ddagger/\Delta G^\ddagger$ in kcal mol⁻¹] for allylic isomerization via TS_{ISO}[**6**] with the [Ni^{II}(η^3 , η^1 (C³), Δ -dodecatrienediyl)] species **6** as precursor.^[a–e]

Isomer of 6 coupling isomer ^[24]	Isomer of 6 coupling isomer ^[24]	TS _{ISO} [6]
η^3 - <i>anti</i> , η^1 (C ³)- <i>syn</i> , Δ - <i>trans</i> →	η^3 - <i>anti</i> , η^1 (C ³)- <i>anti</i> , Δ - <i>trans</i>	20.7/20.0
		19.5/18.9
		16.2/15.7
		15.4/15.0
η^3 - <i>syn</i> , η^1 (C ³)- <i>syn</i> , Δ - <i>trans</i> →	η^3 - <i>syn</i> , η^1 (C ³)- <i>anti</i> , Δ - <i>trans</i>	13.9/13.6
		13.5/13.0
		16.0/15.5
		16.2/16.5

[a] This process is classified according to the butadiene coupling stereoisomers (indicated by its pictorial representation)^[24] involved. The relationship between the butadiene coupling isomers and the stereoisomers of **6** is explicitly given. [b] Total barriers relative to the most stable isomer of **7**; namely [Ni^{II}(bis(η^3 -*anti*), Δ -*trans*-dodecatrienediyl)].^[34] [c] Numbers in italics are the Gibbs free energies. [d] The lowest barrier of the individual stereochemical pathways is in boldface type. [e] Only the stereochemical pathways that involve bis(allyl), Δ -*trans*-dodecatrienediyl species are reported; the complete collection is included in the Supporting Information (Table S5).

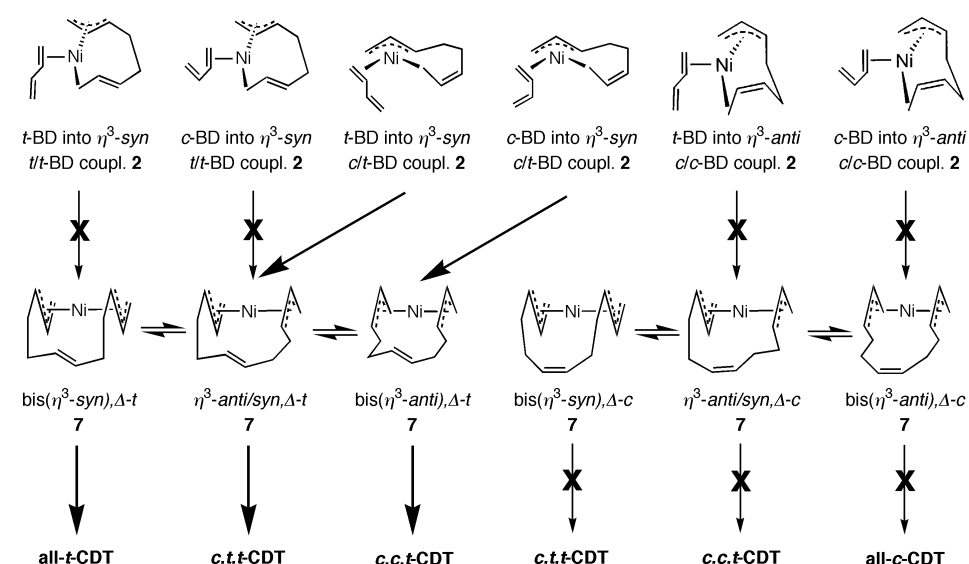
populated (see Section C); thus these compounds are not likely to play any role in the catalytic reaction course. The total barrier for isomerization amounts to 13.0–20.0 kcal mol⁻¹ (ΔG^\ddagger), depending on how efficient the coordinated olefinic double bond could serve to stabilize TS_{ISO}[**6**] for individual stereoisomers. Commencing from the isolated bis(η^3 -*anti*), Δ -*trans* intermediates **7**,^[34] total free-energy barriers of 15.0 kcal mol⁻¹ and 18.9 kcal mol⁻¹ have to overcome,

which can be considered to be large enough to allow isolation of these isomers at low temperature. Overall, the isomerization barrier is predicted to be distinctly lower than the barrier for reductive elimination ($\Delta\Delta G^\ddagger > 5.5$ kcal mol⁻¹, vide infra). This leads to the conclusion, that isomerization via TS_{ISO}[**6**] should be significantly more facile than subsequent reductive elimination; this has been confirmed by NMR investigations of the stoichiometric reaction.^[15] Consequently, the various configurations and stereoisomeric forms of bis(allyl), Δ -*trans*-dodecatrienediyl–Ni^{II} compounds **5–7** are in a kinetically mobile, preestablished equilibrium, with **7** as the prevalent species.

The stoichiometric cyclotrimerization starting from the isolable bis(η^3 -*anti*), Δ -*trans* intermediate has been demonstrated to become accelerated by the presence of donor phosphines (i.e., PMe₃, PEt₃, PPh₃) and also by excess butadiene.^[9a, 16] To clarify the influence of incoming butadiene on the isomerization process several isomers TS_{ISO}[**6**]-**BD**, with a further η^2 -*trans*-butadiene attached, have been located for the most feasible isomerization pathways. All these species are seen to carry a loosely bound butadiene moiety, and are ~ 6.0 kcal mol⁻¹ (ΔH) above the separated species {TS_{ISO}[**6**] + *trans*-butadiene}. Incoming butadiene does not serve to facilitate allylic isomerization by stabilization of TS_{ISO}[**6**], and will therefore not assist this process. Accordingly, reductive elimination must be considered as the critical step for the rationalization of the experimental observation.

E) Reductive elimination under ring closure in dodecatrienediyl–Ni^{II} species: The η^3 , η^1 species **5**, **6** and the bis(η^3) species **7** of the [Ni^{II}(dodecatrienediyl)] complex can conceivably act as the precursors for reductive elimination. Exploration of several routes in a linear-transit approach^[31] clearly demonstrates that the bis(η^3) species **7** is the direct precursor for reductive elimination along the favorable route, giving rise to the [Ni⁰(CDT)] product **8**. The careful investigation of alternative reaction routes gives no indication of the bis(η^1) species being involved along viable routes, which is similar to the findings for the reductive elimination process for the [Ni⁰L]-catalyzed cyclodimerization of butadiene.^[19]

Scheme 2 displays the competing paths for generation of the various isomers of CDT. Clearly, the bis(η^3 -*syn*), Δ -*trans* and bis(η^3 -*anti*), Δ -*cis* isomers of **7** are the precursors for the generation of all-*t*- and all-*c*-CDT, respectively. On the other hand, *c,c,t*- and *c,t,t*-CDT can be formed along alternative paths that involve either bis(η^3 -*allyl*), Δ -*trans* (product of butadiene insertion into the η^3 -*syn*–Ni^{II} bond through **2** → **7**) or bis(η^3 -*allyl*), Δ -*cis* (product of *trans*-butadiene insertion into the η^3 -*anti*–Ni^{II} bond through **2** → **7** followed by facile allylic isomerization via TS_{ISO}[**6**]) precursors **7**. The complete branch for generation of bis(η^3 -*allyl*), Δ -*cis* isomers of **7**, however, is entirely disabled (see Section C) and only bis(η^3 -*allyl*), Δ -*trans* isomers are present in appreciable concentrations. Among the various bis(η^3 -*allyl*), Δ -*trans* isomers of **7**, the η^3 -*syn*/ η^3 -*anti*, Δ -*trans* and bis(η^3 -*anti*), Δ -*trans* isomers, which are the precursors for the *c,t,t*- and *c,c,t*-CDT-generating paths, respectively, are formed in a direct fashion along **2** → **7** (see Section C), while the bis(η^3 -*syn*), Δ -*trans* precursor for the all-*t*-CDT production path is accessible from these isomers by facile



Scheme 2. Competing paths for generation of all-*c*-, *c,c,t*-, *c,t,t*-, and all-*t*-CDT commencing from the oxidative coupling $\eta^3, \eta^1(C^1)$ -octadienediyl- Ni^{II} product species **2**. Butadiene insertion along **2** \rightarrow **7** preferably takes place into the η^3 -allyl- Ni^{II} bond of **2**, and the bis(η^3 -allyl), Δ species **7** is the direct precursor for reductive elimination. (Please note, that only one of the four possible stereoisomeric forms is displayed for each of the given species **2** and **7**)

isomerization of one or both terminal allylic groups via $TS_{ISO}[6]$ (see Section D). The precursors **7** for competing paths for reductive elimination affording *c,c,t*-, *c,t,t*-, and all-*t*-CDT might be populated to a similar amount, since they are close in energy (Table 7). How incoming butadiene or the presence of donor phosphines affect the concentration and the reactivity of the different precursors **7** will be elaborated in the final paragraphs of this section.

Table 7. Activation enthalpies and free energies [$\Delta H^\ddagger/\Delta G^\ddagger$ in kcal mol $^{-1}$] and reaction enthalpies and free energies [$\Delta H/\Delta G$ in kcal mol $^{-1}$] for reductive elimination affording CDT along **7** \rightarrow **8**.^[a-f]

CDT isomer	7	TS[7-8]	8
all- <i>t</i> -CDT	bis(η^3 - <i>syn</i>), Δ - <i>trans</i>		
	3.5/1.7	27.9/27.2	-13.5/-12.9
	5.1/3.1	31.9/32.4	-10.3/-10.0
	5.4/3.8	32.9/32.6	-10.4/-10.2
	5.1/3.1	31.9/32.4	-10.3/-10.0
<i>c,c,t</i> -CDT	bis(η^3 - <i>anti</i>), Δ - <i>trans</i>		
	0.5/0.6	[e]	
	0.0/0.0	[e]	
	2.5/2.5	25.2/25.5	-8.4/-7.6
	2.5/2.5	25.3/25.7	-8.4/-7.7
<i>c,t,t</i> -CDT	η^3 - <i>syn</i> / η^3 - <i>anti</i> , Δ - <i>trans</i>		
	6.7/5.1	31.5/31.3	-9.4/-8.8
	4.3/2.8	36.6/35.6	-9.4/-8.8
	9.0/6.9	38.8/38.2	-6.5/-6.3
	4.0/2.4	26.2/27.1	-9.8/-8.9

[a] This process is classified according to the butadiene coupling stereoisomers (indicated by its pictorial representation)^[24] involved. The relationship between the butadiene coupling isomers and the stereoisomers of **7** and **8** is explicitly given. [b] Total barriers and reaction energies relative to the most stable isomer of **7**; namely $[Ni^{II}(\text{bis}(\eta^3\text{-anti}), \Delta\text{-trans-dodecatrienediyl})]$.^[34] [c] Numbers in italics are the Gibbs free energies. [d] The lowest barrier of the individual stereochemical pathways for formation of *c,c,t*-, *c,t,t*-, and all-*t*-CDT is in boldface type. [e] For this stereoisomer^[34] no facile reductive elimination is possible, see text. [f] Only few of the stereochemical pathways are reported; the complete collection is included in the Supporting Information (Table S6).

The key species involved along the most feasible of the various stereochemical pathways for reductive elimination **7** \rightarrow **8** affording *c,c,t*-, *c,t,t*-, and all-*t*-CDT, respectively, are displayed in Figure 6. Along **7** \rightarrow **8**, the twelve-membered ring is generated by establishing of a C-C σ -bond between the terminal unsubstituted carbons (C^1, C^{12}) of two η^3 -allylic groups in the precursor **7**. The transition state $TS[7-8]$ occurs at a distance of ~ 1.9 – 2.1 Å of the emerging bond and is characterized by a partly η^3 -allyl \rightarrow vinyl conversion of both allylic groups and decays into the formal $16e^-$ planar $[Ni^0(\text{CDT})]$ product **8**, in which CDT is coordinated to nickel by its three olefinic double bonds.

Two different conformations of $TS[7-8]$ have been located. An SP transition state is crossed along the pathway for formation of all-*t*-CDT, in which the *trans* double bond is not coordinated to nickel. On the other hand, the pathways for generation of *c,c,t*- and *c,t,t*-CDT involve a SPY transition state, in which the coordinated *trans* double bond is situated in an axial site (Figure 6).

Commencing from bis(η^3 -allyl), Δ -*trans* isomers of **7**, which serve as a thermodynamic sink due to the highly exogonic insertion, reductive elimination is seen as that crucial elementary step, which is connected with the highest barrier (see Table 7). Thus, reductive elimination along **7** \rightarrow **8** must be considered to be rate-controlling, with the bis(η^3 -allyl), Δ -*trans* precursors are in a kinetically mobile, preestablished equilibrium. Consequently, the selectivity of the CDT formation is kinetically regulated by the difference in the total free-energy of activation ($\Delta\Delta G^\ddagger$, relative to, for example, the most favorable bis(η^3 -*anti*), Δ -*trans* stereoisomer^[34] of the precursor **7**) connected with the competing reductive elimination pathways for generation of *c,c,t*-, *c,t,t*-, and all-*t*-CDT, on account of the Curtin–Hammett principle.^[35]

Starting from the thermodynamically most favorable bis(η^3 -*anti*), Δ -*trans* stereoisomers of **7**, in which the two allylic groups are arranged in opposite orientation,^[34] reductive elimination gives rise to an insurmountable barrier, caused by the *trans* orientation of the reactive terminal allylic carbons. The corresponding $TS[7-8]$ could not be located for these stereoisomers; however, this is expected to be energetically very high. These stereoisomers constitute dead-end points within the catalytic cycle and they first have to undergo allylic isomerization in order to make feasible pathways for reductive elimination accessible, which agrees with experimental observation.^[15]

The all-*t*-CDT-generating path, involving the bis(η^3 -*syn*), Δ -*trans* stereoisomer of **7**, which originates from the linkage of

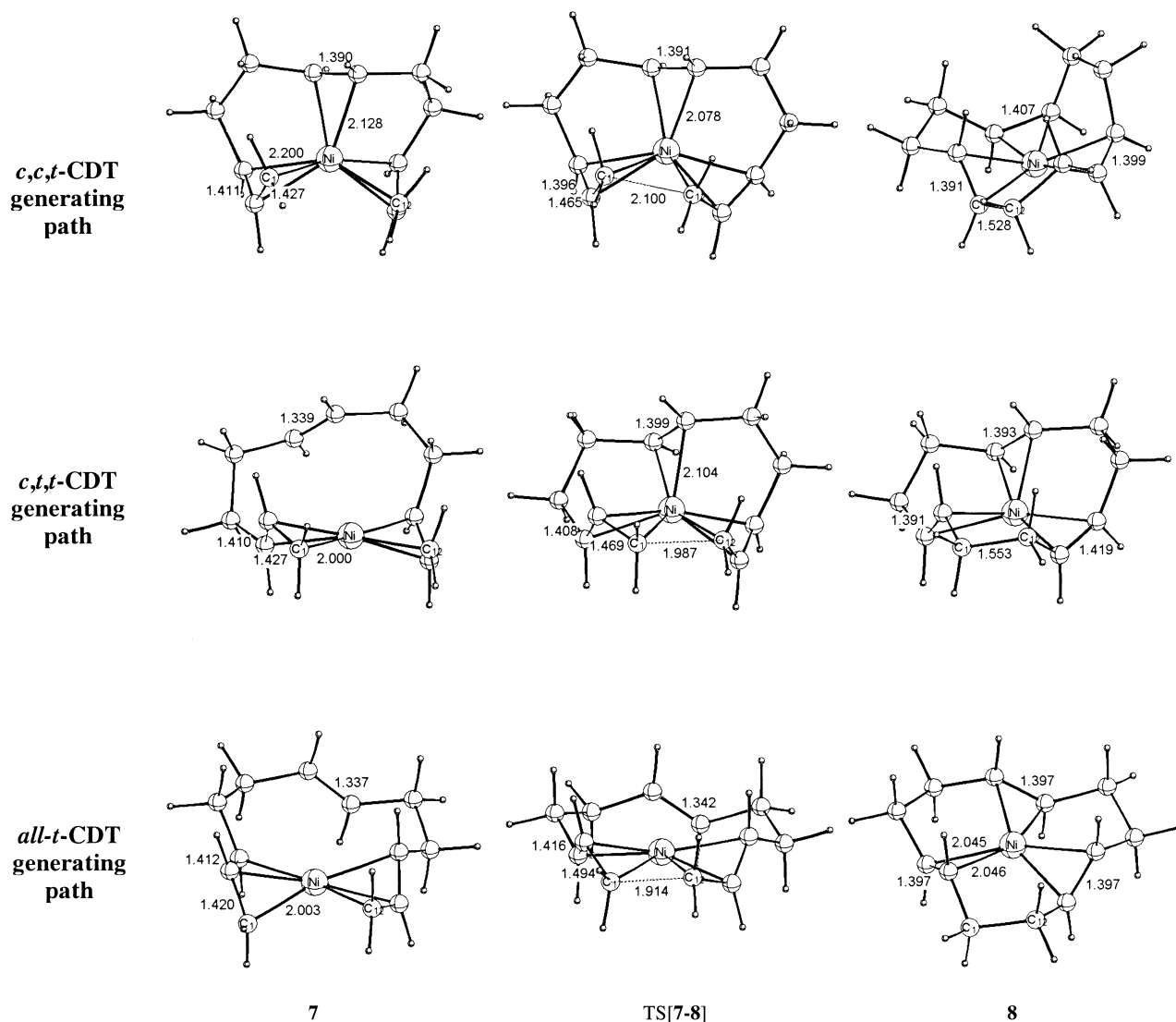


Figure 6. Selected geometric parameters [Å] of the optimized structures of key species for reductive elimination by the most feasible stereochemical pathway for the competing paths affording *c,c,t*-CDT, *c,t,t*-CDT and all-*t*-CDT, respectively, along $7 \rightarrow 8$.

three *trans*-butadienes of identical enantiofaces, is connected with a total free-energy barrier of $27.2 \text{ kcal mol}^{-1}$ (relative to the favorable bis(η^3 -*anti*), Δ -*trans* stereoisomer^[34] of **7**, see Table 7). This leads to the thermodynamically most favorable [Ni⁰(all-*t*-CDT)] compound of all product species **8**,^[36] in a process that is $-12.9 \text{ kcal mol}^{-1}$ exergonic (ΔG). The calculated geometry for the [Ni⁰(all-*t*-CDT)] product **8** is in excellent agreement with available X-ray data.^[17c] All-*t*-CDT is liberated through subsequent, consecutive substitution steps with butadiene in an overall exothermic process ($\Delta H = -8.6 \text{ kcal mol}^{-1}$), which regenerates the active catalyst **1b**.

The most feasible of the various stereochemical pathways for formation of *c,c,t*-CDT, which involves the bis(η^3 -*anti*), Δ -*trans* precursor **7**,^[37a] has a total free-energy barrier of $25.5 \text{ kcal mol}^{-1}$, and along the favorable stereochemical pathway for the *c,t,t*-CDT-generating path starting from the η^3 -*syn*/ η^3 -*anti*, Δ -*trans* species **7**,^[37b] a total free-energy barrier of $27.1 \text{ kcal mol}^{-1}$ (Table 7) has to be overcome. The corresponding products **8**, that are formed in moderately exergonic

processes, are thermodynamically less favorable compared to the [Ni⁰(all-*t*-CDT)] product.^[36] It is interesting to note, that the entirely disabled route for the formation of all-*c*-CDT (see Section C) would also require the highest total barrier for reductive elimination (see Table S6 in the Supporting Information). The total kinetic barrier for reductive elimination along competing paths for generation of *c,c,t*-, *c,t,t*-, and all-*t*-CDT indicates the first path to be most facile. This would suggest that *c,c,t*-CDT should be formed as the predominant C₁₂-cycloolefin, with *c,t,t*-CDT and all-*t*-CDT generated in minor, but similar, portions, which is contrary to the observed selectivity of the catalytic cyclotrimerization.

The role played by incoming butadiene on thermodynamic and kinetic aspects of the rate-determining reductive elimination step $7 \rightarrow 8$ will be clarified in further discussion. First, several [Ni^{II}(dodecatrienediyl)(η^2 -*trans*-butadiene)] precursor species have been located for the most feasible pathways of the three competing CDT-generating paths. The incoming butadiene has to compete for coordination with the possibly coordinated olefinic double bond of the C₁₂ chain. The bis(η^3 -

syn), Δ -*trans* precursor for the all-*t*-CDT production path, in which the *trans* double bond is not coordinated to nickel (Figure 6) displays the highest tendency to coordinate an additional butadiene in an axial site, while the corresponding precursors involved along the *c,c,t*- and *c,t,t*-CDT-generating paths are characterized by loosely bound butadiene and double bond moieties; thus indicating no notable tendency for butadiene coordination. All localized [Ni^{II}(dodecatrienediyl)(η^2 -*trans*-butadiene)] compounds are found to be higher in enthalpy relative to the separated fragments, which amounts to 5.5 kcal mol⁻¹ (ΔH) for the bis(η^3 -*syn*), Δ -*trans* precursor. This indicates that the coordination of incoming butadiene in dodecatrienediyl–Ni^{II} species is not a likely process. Therefore, the species **7** are the predominant precursor species for reductive elimination, with the corresponding butadiene adducts, **7-BD**, expected to be negligibly populated. Incoming butadiene does not serve to displace the equilibrium between the precursors of the three competing CDT paths.

Coordination of butadiene in TS[**7-8**] is seen to go at the expense of the coordinated olefinic double bond in the SPY transition-states for the *c,c,t*- and *c,t,t*-CDT-generating paths. The coordinated *trans* double bond cannot compete for coordination with the incoming butadiene and becomes displaced by η^2 -*trans*-butadiene in TS[**7-8**]-**BD**. Although coordination of free butadiene is more favorable than coordination of the *trans* double bond from the C₁₂ chain, it can only partially compensate for the deformation of the C₁₂ chain. The total enthalpic barrier (relative to the separated most favorable bis(η^3 -*anti*), Δ -*trans* stereoisomer^[34] and *trans*-butadiene) via TS[**7-8**]-**BD** amounts to 30.0 and 22.0 kcal mol⁻¹ (ΔH^\ddagger) for the *c,c,t*- and *c,t,t*-CDT-generating paths, respectively, which have to be compared with the barriers of 25.2 and 26.2 kcal mol⁻¹ (ΔH^\ddagger), respectively (Table 7), predicted for the process not assisted by incoming butadiene. The *c,c,t*-CDT-generating path is clearly not indicated to be kinetically facilitated under the influence of additional butadiene. Also, the enthalpic stabilization of the transition state for the *c,t,t*-CDT path ($\Delta\Delta H^\ddagger = 4.2$ kcal mol⁻¹) does not seem to be large enough to compensate for the entropic cost of monomer coordination.^[26, 38] Overall, it must be concluded, that the *c,c,t*- and *c,t,t*-CDT-generating paths are not likely to be assisted by incoming butadiene.^[38b]

In contrast, the SP transition state involved along the all-*t*-CDT-generating path is substantially stabilized by coordination of new butadiene (Figure 7). The total enthalpic barrier of 27.9 kcal mol⁻¹ (Table 7) for **7** \rightarrow **8** is lowered by 9.8 kcal mol⁻¹ ($\Delta\Delta H^\ddagger$) for the process, in which incoming butadiene participates ($\Delta H^\ddagger = 18.1$ kcal mol⁻¹). Taking the reasonably guessed entropic cost of ~ 5 kcal mol⁻¹ for monomer association into account,^[38a] indicates that the all-*t*-CDT-generating path becomes facilitated by incoming monomer as well at the free-energy surface (ΔG). The *trans*-butadiene adduct of the [Ni⁰(all-*t*-CDT)] product **8-BD**, however, lies 1.0 kcal mol⁻¹ (ΔH) above the separated fragments; this is not unexpected for the weak donor butadiene. Thus, incoming butadiene is seen to stabilize the transition state for the all-*t*-CDT path, but the monomer is not likely to assist the process at the very early and the very late stages.

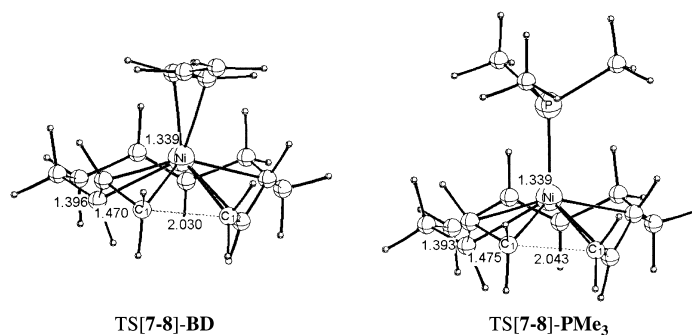


Figure 7. Selected geometric parameters [Å] of the optimized transition-state structure TS[**7-8**] for reductive elimination along the all-*t*-CDT-generating path, assisted by *trans*-butadiene and PMe₃, respectively.

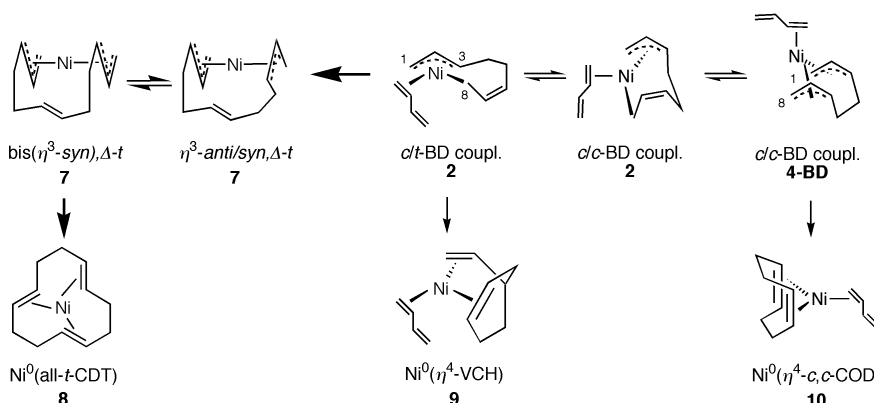
How the presence of donor phosphines influences the reductive elimination step has also been examined, with PMe₃ chosen as a suitable model. Similar to the findings discussed above, PMe₃ adducts of **7** are predicted to be negligibly populated, with **7** representing the predominant form of the precursor species. Furthermore, the path for generation of all-*t*-CDT is the only path, that becomes kinetically favored by phosphine coordination. Compared with butadiene, the stronger donor PMe₃ serves to stabilize the productlike quasi-tetrahedral transition state with axial ligand coordination, as well as the product to a larger extent. The total enthalpic barrier (relative to the separated most favorable bis(η^3 -*syn*), Δ -*trans* stereoisomer^[34] and PMe₃) is reduced by 11.9 kcal mol⁻¹ and the pseudotetrahedral [Ni⁰(all-*t*-CDT)PMe₃] product, for which the optimized geometry perfectly matches available X-ray data,^[18] is 9.8 kcal mol⁻¹ (ΔH) below the separated fragments.^[39]

To summarize, the reductive elimination paths affording *c,c,t*- and *c,t,t*-CDT are neither assisted by incoming butadiene nor by the presence of PR₃ ligands. However, butadiene as well as donor phosphines are indicated to serve to kinetically facilitate the all-*t*-CDT-generating path. Comparison of the total free-energy barriers for the paths affording all-*t*-CDT (18.1 + 5 \approx 23 kcal mol⁻¹ via TS[**7-8**]-**BD**), *c,c,t*-CDT (25.5 kcal mol⁻¹ via TS[**7-8**]), and *c,t,t*-CDT (27.1 kcal mol⁻¹ via TS[**7-8**]) indicates the all-*t*-CDT path to be the most facile of the competing CDT production paths. The difference in the total free-energy of activation ($\Delta\Delta G^\ddagger$) of more than ~ 2.5 kcal mol⁻¹ between the favorable all-*t*-CDT-generating path and the *c,c,t*- and *c,t,t*-CDT paths suggests that all-*t*-CDT should predominantly be formed together with smaller portions of *c,c,t*-CDT and *c,t,t*-CDT; this is consistent with experiment.^[9a]

F) Competition between reaction channels for formation of C₈- and C₁₂-cycloolefins:

The discussion of critical aspects of the reaction mechanism so far has entirely been focused on the reaction channel for the generation of C₁₂-cycloolefin products. Although C₁₂-cycloolefins are the predominant products, a minor portion of C₈-cycloolefins ($\sim 5\%$) is also formed in the catalytic process.^[9a] It has been demonstrated in our previous theoretical exploration of the [Ni⁰L]-catalyzed cyclodimerization,^[19] that 1) the [Ni^{II}(octadienediyl)L] complex represents the crucial species for the formation of the two

major 4-vinylcyclohexene (VCH) and *cis,cis*-cycloocta-1,5-diene (*cis,cis*-COD) C₈-cycloolefin products along competing paths for the rate-determining reductive elimination step, and 2) the η^3,η^1 - and bis(η^3)-octadienediyl–Ni^{II} species act as the respective precursors. Consequently, the [Ni^{II}(η^3,η^1 (C¹)-octadienediyl)(η^2 -butadiene)] species **2** is likely to represent the critical species that connects the alternative reaction channels for formation of either C₁₂- or C₈-cycloolefins (Scheme 3). As discussed in Section C the C₁₂-cyclotrimer channel is entered through butadiene insertion into the η^3 -allyl–Ni^{II} bond along the **2** → **7** path. The channel for generation of C₈-cyclodimer products is accessible through intramolecular C–C bond formation in the octadienediyl–Ni^{II} framework by reductive



Scheme 3. Two reaction channels for generation of cyclodimer and cyclotrimer products in the Ni⁰-catalyzed cyclooligomerization of 1,3-butadiene.

elimination under ring closure, with the η^2 -butadiene serving to act as a spectator ligand; namely between the substituted C³ of the η^3 -allylic moiety and the terminal C⁸ of the η^1 -allylic moiety in **2**, giving rise to the [Ni⁰(η^4 -VCH)(η^2 -butadiene)] product **9**, and between the terminal unsubstituted C¹ and C⁸ of both η^3 -allylic moieties in the bis(η^3) species **4-BD**; this affords the [Ni⁰(η^4 -*cis,cis*-COD)(η^2 -butadiene)] product **10**.^[19]

The species **2** and **4-BD** are in a preestablished equilibrium, thus for this typical Curtin–Hammett situation^[35] the C₈:C₁₂ product ratio is entirely regulated by the difference in the free-energy of activation ($\Delta\Delta G^\ddagger$) between the elimination routes **2** → **9** and **4-BD** → **10**, and the **2** → **7** butadiene insertion route (cf. Scheme 3). Formation of VCH and *cis,cis*-COD along the most feasible stereochemical pathway for **2** → **9** (coupling product of two *cis*-butadienes of identical enantiofaces)^[19] and for **4-BD** → **10** (which involves the coupling product of two *cis*-butadienes of opposite enantiofaces)^[19] is connected with total barriers of 17.2 kcal mol⁻¹ and 16.8 (ΔG^\ddagger), respectively, relative to the thermodynamically most favorable η^3 -syn, η^1 (C¹),Δ-*cis* stereoisomer of **2**. On the other hand, butadiene insertion along **2** → **7** requires a total free-energy barrier of 14.0 kcal mol⁻¹ (Section C). Hence, the C₁₂-cyclotrimer-generating reaction channel is favored, while the reaction channel for production of C₈-cyclodimers is kinetically retarded by higher barriers of 2.8–3.2 kcal mol⁻¹ ($\Delta\Delta G^\ddagger$). In agreement with experiment,^[9a] C₁₂-cycloolefins, with all-*t*-CDT as the predominant isomer, are indicated to be

the major products of the Ni⁰-catalyzed cyclooligomerization of 1,3-butadiene, and C₈-cycloolefins, with VCH and *cis,cis*-COD, which are expected to be generated in similar amounts, formed in minor portions.

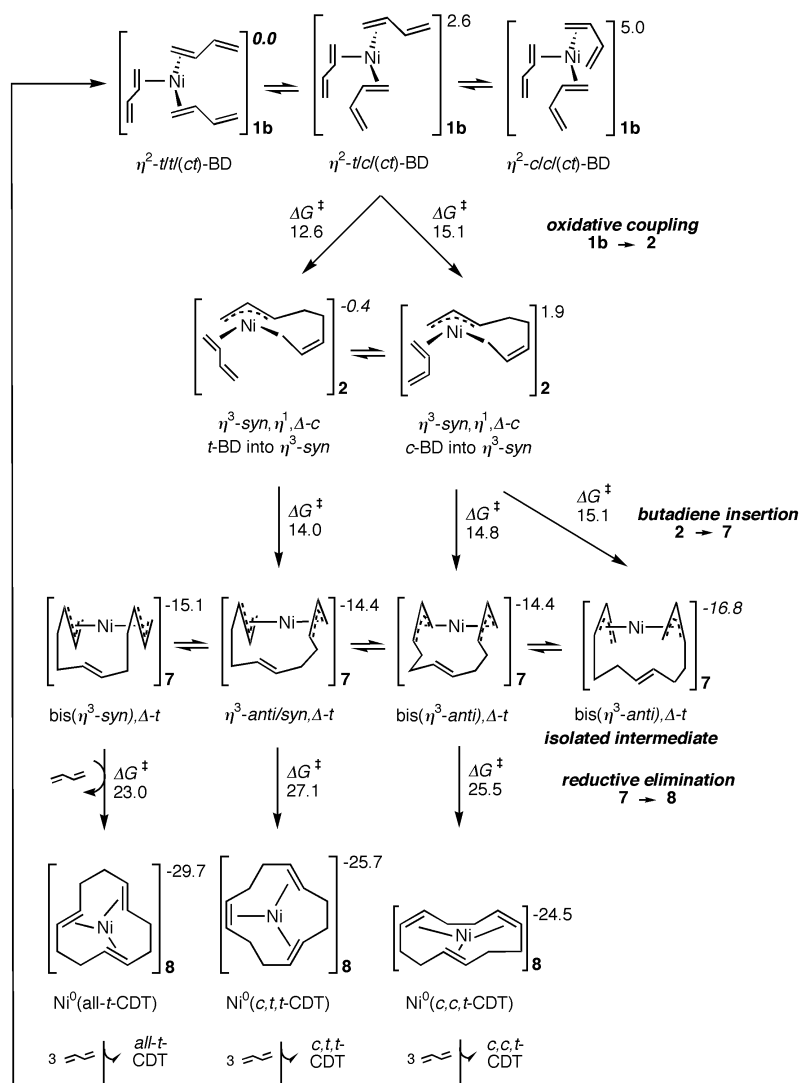
Conclusions

A comprehensive theoretical investigation of the mechanism for the Ni⁰-catalyzed cyclotrimerization of 1,3-butadiene has been presented, employing a gradient-corrected DFT method. Important elementary processes of the entire catalytic cycle with the [Ni⁰(η^2 -butadiene)₃] complex acting as active catalyst have been scrutinized, namely, oxidative coupling of two butadienes, butadiene insertion into the allyl–Ni^{II} bond, allylic isomerization in both the octadienediyl–Ni^{II} and dodecatrienediyl–Ni^{II} complexes, and reductive elimination under ring closure. For each of these elementary steps several conceivable routes and also the different stereochemical pathways have been probed. Based on this work, a condensed mechanistic scheme for the complete cycle of the Ni⁰-catalyzed cyclotrimerization of 1,3-butadiene is presented, consisting of the most feasible routes for the important elementary reaction processes (Scheme 4).

Overall, the cyclotrimerization process is driven by a strong thermodynamic force with an exothermicity of –44.6 kcal mol⁻¹ (ΔH for the process without a catalyst) for the fusion of three *trans*-butadienes to afford the favorable all-*t*-CDT isomer.

Among the various forms, the formal 16e⁻ trigonal planar [Ni⁰(η^2 -butadiene)₃] form of **1b**, with the tris(η^2 -*trans*-butadiene) isomer most favorable, is most likely to be the prevalent species of the active catalyst. Complex **1b** is also shown to represent the precursor for the favorable **1b** → **2** route for oxidative coupling between the terminal non-coordinated carbons of two reactive η^2 -butadiene moieties; this is assisted by an ancillary butadiene in the η^2 -mode. The most feasible stereochemical pathway takes place through the coupling of η^2 -*trans*/ η^2 -*cis* butadiene moieties (of opposite enantioface) with the lowest barrier of 12.6 kcal mol⁻¹ (ΔG^\ddagger). This gives rise to the most favorable isomer of the initial η^3,η^1 (C¹)-octadienediyl–Ni^{II} coupling product **2** in an almost thermoneutral process, indicating the oxidative coupling to be reversible. The same stereochemical pathway has been shown to be favorable for the oxidative coupling step for the [Ni⁰L]-catalyzed cyclodimerization reaction.^[19] Alternative pathways for coupling of two *cis*-butadiene or two *trans*-butadiene moieties are unfeasible.

The dominant dodecatrienediyl–Ni^{II} formation path occurs due to insertion of butadiene into the η^3 -allyl–Ni^{II} bond of the



Scheme 4. Condensed Gibbs free-energy profile [kcal mol⁻¹] of the entire catalytic cycle of the Ni⁰-catalyzed cyclotrimerization of 1,3-butadiene, focused on viable routes for individual elementary steps. The favorable [Ni⁰(η^3 -*trans*-butadiene)₃] isomer of the active catalyst species **1b** was chosen as reference, and the activation barriers for individual steps are given relative to the favorable isomer of the respective precursor (marked in italics).

initial coupling product **2**. Similar activation barriers of 14.0–15.1 kcal mol⁻¹ (ΔG^\ddagger) have to be overcome along the most feasible pathway for *trans*- and *cis*-butadiene insertion into the η^3 -*syn*-Ni^{II} bond, giving rise to η^3 -*syn*/ η^3 -*anti*, Δ -*trans* and bis(η^3 -*anti*), Δ -*trans* isomers of **7**. Butadiene is inserted irreversibly into the η^3 -allyl-Ni^{II} bond along **2** \rightarrow **7** in a highly exogonic process of ~ -15 to -20 kcal mol⁻¹ (ΔG). The most favorable bis(η^3), Δ -dodecatrienediyl-Ni^{II} species **7** serves, therefore, as a thermodynamic sink. Identical butadiene coupling stereoisomers (*trans/cis*-butadiene coupling) are involved along the most feasible pathways for the oxidative coupling of **1b** \rightarrow **2** and butadiene insertion of **2** \rightarrow **7**. Thus, allylic isomerization in the octadienediyl-Ni^{II} complex via TS_{ISO}[**3**] is not a necessary process in the catalytic reaction course.

The complete branch for formation of bis(η^3 -allyl), Δ -*cis*-dodecatrienediyl-Ni^{II} isomers of **7**, which are the precursor

for the all-*c*-CDT-generating path, is disabled, first because of the unfavorable coupling of the two *cis*-butadiene moieties along **1b** \rightarrow **2** together with a slow isomerization via η^3 -*anti*, η^1 (C³) isomers of TS_{ISO}[**3**] (this prevents an appreciable concentration of *cis/cis*-butadiene coupling η^3 -*anti*, η^1 (C¹), Δ -*cis* isomers of **2**), and second as a result of the kinetically impeded butadiene insertion into the η^3 -*anti*-allyl-Ni^{II} bond along **2** \rightarrow **7**. Consequently, the all-*c*-CDT-generating path is completely precluded.

The thermodynamically highly favored bis(η^3 -allyl), Δ -*trans*-dodecatrienediyl-Ni^{II} form of **7** is the direct precursor for reductive elimination, which involves the overall largest kinetic barrier among all crucial elementary steps and gives rise to the [Ni⁰(CDT)] product **8** in an exogonic irreversible process. Thus, reductive elimination along **7** \rightarrow **8** is predicted to be rate-controlling. The cyclotrimer products are liberated in subsequent, consecutive substitution steps with butadiene, which is exothermic by -8.6 kcal mol⁻¹ (ΔH) for expulsion of all-*t*-CDT by three *trans*-butadienes along **8** \rightarrow **1b**. This process, however, is endergonic by ~ 7 kcal mol⁻¹ (ΔG) taking reasonably estimated entropic costs into account.^[38a] Therefore, **7** and **8** (stabilized by donors)

are indicated to be likely candidates for isolable intermediates of the catalytic process, while the active catalyst **1** and other species are either too reactive or not present in appreciable concentration for experimental characterization.

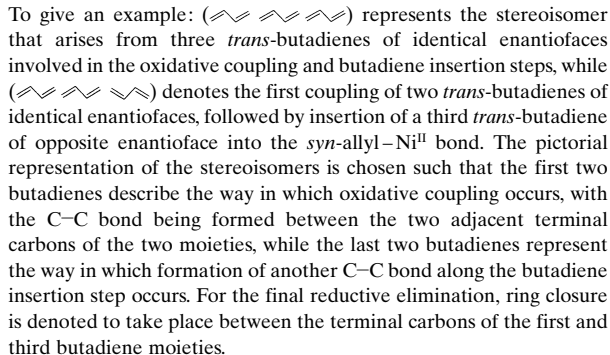
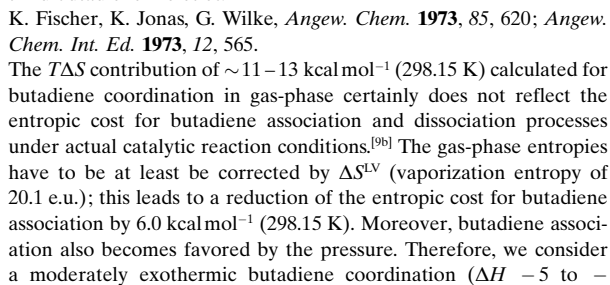
The various isomers of CDT are formed along competing paths for reductive elimination **7** \rightarrow **8** with the bis(η^3 -*anti*), Δ -*trans* and η^3 -*syn*/ η^3 -*anti*, Δ -*trans* isomers of **7**, which are formed along feasible pathways for **2** \rightarrow **7**, acting as precursors for the *c,c,t*-CDT- and *c,t,t*-CDT-generating paths, respectively. The bis(η^3 -*syn*), Δ -*trans* precursor for the all-*t*-CDT path is readily formed from the direct accessible isomers of **7** through facile allylic isomerization via TS_{ISO}[**6**]. Thus the various bis(η^3 -allyl), Δ -*trans* precursors **7** are in a kinetically mobile, pre-established equilibrium and are predicted to exist in similar concentration. Incoming butadiene does not serve to displace the equilibrium between the precursors. Accordingly, the selectivity of the CDT formation is regulated by the difference

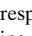
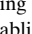
in the total free-energy barrier ($\Delta\Delta G^\ddagger$) for the three competing paths.

The *c,c,t*-CDT and *c,t,t*-CDT production paths are shown not to be assisted by incoming butadiene, while the SP transition state for generation of all-*t*-CDT is significantly stabilized by a axial coordinated η^2 -*trans*-butadiene. Hence, the all-*t*-CDT path becomes the most facile of the three competing paths with a total free-energy barrier for reductive elimination of ~ 23 kcal mol⁻¹.^[40] Thus, moderate reaction conditions^[9] are required for the catalytic cyclotrimerization, although **7** represents a thermodynamic sink within the catalytic cycle. All-*t*-CDT is predicted to be formed as the predominant C₁₂-cycloolefin, together with significantly smaller amounts of *c,c,t*-CDT and *c,t,t*-CDT, since their generation is kinetically impeded by reductive elimination barriers that are more than ~ 2.5 kcal mol⁻¹ ($\Delta\Delta G^\ddagger$) higher. Furthermore, the formation of minor portions of C₈-cycloolefins is rationalized.

Acknowledgement

The author is grateful to Prof. Dr. Rudolf Taube for his ongoing interest in this research, which is a continual stimulus. The author is furthermore indebted to Prof. Dr. Reinhart Ahlrichs (University of Karlsruhe, Germany) for making the latest version of Turbomole available. Excellent service by the computer centers URZ Magdeburg and URZ Halle is gratefully acknowledged. The author wish to thank the Deutsche Forschungsgemeinschaft (DFG) for financial support by an Habilitandenstipendium.

- [1] a) "The Oligomerization and Co-oligomerization of Butadiene and Substituted 1,3-Dienes": P. W. Jolly, G. Wilke in *The Organic Chemistry of Nickel, Vol. 2, Organic Synthesis*, Academic Press, New York, **1975**, pp. 133–212; b) "Nickel-Catalyzed Oligomerization of 1,3-Dienes and Related Reactions": P. W. Jolly in *Comprehensive Organometallic Chemistry, Vol. 8* (Eds.: G. Wilkinson, F. G. A. Stone, E. W. Abel), Pergamon, New York, **1982**, pp. 671–711.
- [2] a) G. Wilke, *Angew. Chem.* **1957**, *69*, 397; b) H. Breil, P. Heimbach, M. Kröner, H. Müller, G. Wilke, *Makromol. Chem.* **1963**, *69*, 18.
- [3] a) G. Wilke, *Angew. Chem.* **1963**, *75*, 10; *Angew. Chem. Int. Ed. Engl.* **1963**, *2*, 105; b) G. Wilke *Angew. Chem.* **1988**, *100*, 189; *Angew. Chem. Int. Ed. Engl.* **1988**, *27*, 185; c) "Cyclooligomerizations and Cyclo-Co-Oligomerizations of 1,3-Dienes": G. Wilke, A. Eckerle in *Applied Homogeneous Catalysis with Organometallic Complexes* (Eds.: B. Cornils, W. A. Herrmann), VCH, Weinheim, Germany, **1996**, pp. 358–373.
- [4] a) G. Schomburg, D. Henneberg, P. Heimbach, E. Janssen, H. Lehmkuhl, G. Wilke, *Liebigs Ann. Chem.* **1975**, 1667; b) P. Heimbach, *Aspects Homogeneous Catal.* **1977**, *2*, 81.
- [5] H. W. B. Reed, *J. Chem. Soc.* **1954**, 1931.
- [6] a) G. Wilke, *Pure Appl. Chem.* **1978**, *50*, 677; b) G. Wilke, *J. Organomet. Chem.* **1980**, *200*, 349.
- [7] G. Wilke, M. Kröner, B. Bogdanovic, *Angew. Chem.* **1961**, *73*, 755.
- [8] G. Wilke, E. W. Müller, M. Kröner, P. Heimbach, H. Breil, DBP 1191375 (Prior. 28. 4.), **1960**.
- [9] a) B. Bogdanovic, P. Heimbach, M. Kröner, G. Wilke, *Liebigs Ann. Chem.* **1969**, *727*, 143; b) the catalytic cyclotrimerization has been performed under the following conditions: 40–80 °C in liquid butadiene under pressure.
- [10] P. W. Jolly, R. Mynott, R. Salz, *J. Organomet. Chem.* **1980**, *184*, C49.
- [11] P. W. Jolly, R. Mynott, *Adv. Organomet. Chem.* **1981**, *19*, 257.
- [12] a) R. Benn, B. Büssemeier, S. Holle, P. W. Jolly, R. Mynott, I. Tkatchenko, G. Wilke, *J. Organomet. Chem.* **1985**, *279*, 63; b) P. W. Jolly, I. Tkatchenko, G. Wilke, *Angew. Chem.* **1971**, *83*, 329; *Angew. Chem. Int. Ed. Engl.* **1971**, *10*, 329; c) J. M. Brown, B. T. Golding, M. J. Smith, *J. Chem. Soc. Chem. Commun.* **1971**, 1240; d) B. Barnett, B. Büssemeier, P. Heimbach, P. W. Jolly, C. Krüger, I. Tkatchenko, G. Wilke, *Tetrahedron Lett.* **1972**, 1457.
- [13] Bis(η^1) species of these complexes have never been experimentally characterized. As revealed from our previous theoretical investigation of the cyclodimerization process,^[19] bis(η^1) species of the [Ni^{II}(octadienediyl)PR₃] complex are at very high energies. The donor ability of the PR₃ ligand was shown to be the critical stabilizing factor. Bis(η^1) species are expected to be energetically above and well separated from corresponding η^3, η^1 and bis(η^3) species for the weak donor butadiene. Hence, bis(η^1) species should not be involved along viable pathways for any of the individual elementary steps. Although not explicitly examined, there is no indication for the participation of bis(η^1) species along any of the investigated paths.
- [14] B. Henc, P. W. Jolly, R. Salz, G. Wilke, R. Benn, E. G. Hoffmann, R. Mynott, G. Schroth, K. Seevogel, J. C. Sekutowski, C. Krüger, *J. Organomet. Chem.* **1980**, *191*, 425.
- [15] B. Henc, P. W. Jolly, R. Salz, S. Stobbe, G. Wilke, R. Benn, R. Mynott, K. Seevogel, R. Goddard, C. Krüger, *J. Organomet. Chem.* **1980**, *191*, 449.
- [16] G. Wilke, E. W. Müller, M. Kröner, *Angew. Chem.* **1961**, *73*, 33.
- [17] a) G. Wilke, *Angew. Chem.* **1960**, *72*, 581; b) H. Dietrich, H. Schmidt, *Naturwissenschaften* **1965**, *52*, 301; c) D. J. Brauer, C. Krüger, *J. Organomet. Chem.* **1972**, *44*, 397; d) K. Jonas, P. Heimbach, G. Wilke, *Angew. Chem.* **1968**, *80*, 1033; *Angew. Chem. Int. Ed. Engl.* **1968**, *7*, 949.
- [18] E. G. Hoffmann, P. W. Jolly, A. Küsters, R. Mynott, G. Wilke, *Z. Naturforsch. Teil B* **1976**, *31*, 1712.
- [19] a) S. Tobisch, T. Ziegler, *J. Am. Chem. Soc.* **2002**, *124*, 4881. b) S. Tobisch, T. Ziegler, *J. Am. Chem. Soc.* **2002**, *124*, 13290.
- [20] a) R. Ahlrichs, M. Bär, M. Häser, H. Horn, C. Kölmel, *Chem. Phys. Lett.* **1989**, *162*, 165 (current version: <http://www.chemie.uni-karlsruhe.de/PC/TheoChem>); b) O. Treutler, R. Ahlrichs, *J. Chem. Phys.* **1995**, *102*, 346; c) K. Eichkorn, O. Treutler, H. Öhm, M. Häser, R. Ahlrichs, *Chem. Phys. Lett.* **1995**, *242*, 652.
- [21] a) P. A. M. Dirac, *Proc. Cambridge Philos. Soc.* **1930**, *26*, 376; b) J. C. Slater, *Phys. Rev.* **1951**, *81*, 385; c) S. H. Vosko, L. Wilk, M. Nussiar, *Can. J. Phys.* **1980**, *58*, 1200; d) A. D. Becke, *Phys. Rev. A* **1988**, *38*, 3098; e) J. P. Perdew, *Phys. Rev. B* **1986**, *33*, 8822; f) J. P. Perdew, *Phys. Rev. B* **1986**, *34*, 7406.
- [22] a) F. Bernardi, A. Bottoni, M. Calcinari, I. Rossi, M. A. Robb, *J. Phys. Chem.* **1997**, *101*, 6310; b) V. R. Jensen, K. Børve, *J. Comput. Chem.* **1998**, *19*, 947.
- [23] a) A. H. J. Wachters, *J. Chem. Phys.* **1970**, *52*, 1033; b) P. J. Hay, *J. Chem. Phys.* **1977**, *66*, 4377; c) N. Godbout, D. R. Salahub, J. Andzelm, E. Wimmer, *Can. J. Chem.* **1992**, *70*, 560; d) TURBOMOLE basis set library.
- [24] To give an example:  represents the stereoisomer that arises from three *trans*-butadienes of identical enantiofaces involved in the oxidative coupling and butadiene insertion steps, while  denotes the first coupling of two *trans*-butadienes of identical enantiofaces, followed by insertion of a third *trans*-butadiene of opposite enantioface into the *syn*-allyl–Ni^{II} bond. The pictorial representation of the stereoisomers is chosen such that the first two butadienes describe the way in which oxidative coupling occurs, with the C–C bond being formed between the two adjacent terminal carbons of the two moieties, while the last two butadienes represent the way in which formation of another C–C bond along the butadiene insertion step occurs. For the final reductive elimination, ring closure is denoted to take place between the terminal carbons of the first and third butadiene moieties.
- [25] K. Fischer, K. Jonas, G. Wilke, *Angew. Chem.* **1973**, *85*, 620; *Angew. Chem. Int. Ed.* **1973**, *12*, 565.
- [26] The $T\Delta S$ contribution of ~ 11 – 13 kcal mol⁻¹ (298.15 K) calculated for butadiene coordination in gas-phase certainly does not reflect the entropic cost for butadiene association and dissociation processes under actual catalytic reaction conditions.^[9b] The gas-phase entropies have to be at least be corrected by ΔS^{LV} (vaporization entropy of 20.1 e.u.); this leads to a reduction of the entropic cost for butadiene association by 6.0 kcal mol⁻¹ (298.15 K). Moreover, butadiene association also becomes favored by the pressure. Therefore, we consider a moderately exothermic butadiene coordination (ΔH –5 to –

- 6 kcal mol⁻¹) to be able to compensate for entropic costs; thus, in these cases butadiene complexation would be likely to occur under actual catalytic conditions.
- [27] The ancillary butadiene's enantioface participating in oxidative coupling along **1b** → **2** affects the energetics by less than 0.5 kcal mol⁻¹, and hence will not be stressed in further discussions.
- [28] J. Lukas, P. W. N. M. van Leeuwen, H. C. Volger, A. P. Kouwenhoven, *J. Organomet. Chem.* **1973**, *47*, 153.
- [29] a) J. W. Faller, M. E. Thomsen, M. J. Mattina, *J. Am. Chem. Soc.* **1971**, *93*, 2642; b) K. Vrieze in *Dynamic Nuclear Magnetic Resonance Spectroscopy* (Eds.: L. M. Jackman, F. A. Cotton) Academic Press, New York, **1975**, pp. 441–487.
- [30] S. Tobisch, R. Taube, *Organometallics* **1999**, *18*, 3045.
- [31] In the linear transit approach, the distance of the two carbons of the newly formed C–C σ -bond is chosen as the reaction coordinate.
- [32] a) S. Tobisch, *Acc. Chem. Res.* **2002**, *35*, 96; b) S. Tobisch, *Chem. Eur. J.* **2002**, *8*, 4756; c) S. Tobisch, unpublished results.
- [33] a) S. Lieber, M.-H. Prosenc, H.-H. Brintzinger, *Organometallics* **2000**, *19*, 377; b) P. M. Margl, T. K. Woo, T. Ziegler, *Organometallics* **1998**, *17*, 4997.
- [34] The two stereoisomeric forms of the bis(η^3 -anti), Δ -trans intermediate **7** confirmed by NMR spectroscopy correspond to the () and () butadiene coupling isomers. The first is equivalent to the major stereoisomer (established by NMR spectroscopy)^[11,14] with a parallel orientation of the olefinic double bond, while the second corresponds to the minor stereoisomer with a nonparallel double bond arrangement. We predict the two stereoisomers to be very close in free energy. Different from experimental observation, the stereoisomer with a non-parallel double bond is favorable by 0.6 kcal mol⁻¹ (ΔG).
- [35] a) J. I. Seemann, *Chem. Rev.* **1983**, *83*, 83; b) J. I. Seemann, *J. Chem. Educ.* **1986**, *63*, 42.
- [36] For free CDT as well as for the [Ni⁰(CDT)] complex, the all-*t* isomer is thermodynamically most favorable. For the [Ni⁰(CDT)] complex **8**, the *c,t,t*-CDT and *c,c,t*-CDT isomers are 4.0 and 5.2 kcal mol⁻¹ higher in free energy, respectively, while the thermodynamically least stable all-*c*-CDT isomer is 6.6 kcal mol⁻¹ (ΔG) above the all-*t*-CDT isomer (Table S6 in the Supporting Information). The thermodynamic driving force for the displacement of all-*t*-CDT by all-*c*-CDT in the [Ni⁰(CDT)] complex is -4.9 kcal mol⁻¹ (ΔG), which confirms experimental observation.^[17d]
- [37] Isomers of **7** with identical or different configurations of the two η^3 -allylic groups could serve as precursors for formation of *c,c,t*-CDT and *c,t,t*-CDT (Scheme 2). The following conclusions (cf. Table S6 in the Supporting Information) could be drawn under the assumption that bis(η^3 -allyl), Δ -*cis* species **7** are present in appreciable concentrations; however, this does not match the real catalytic situation; a) The most feasible pathway for *c,c,t*-CDT formation involves bis(η^3 -anti), Δ -*trans* precursors, while the alternative pathway with η^3 -syn/ η^3 -anti, Δ -*cis* species is kinetically disfavored by a barrier that is 3.2 kcal mol⁻¹ (ΔG^\ddagger) larger; b) the η^3 -syn/ η^3 -anti, Δ -*trans* species is the precursor for *c,t,t*-CDT generation along the most feasible pathway, while the transition state along the pathway that involves bis(η^3 -syn), Δ -*cis* precursors lies 2.9 kcal mol⁻¹ (ΔG^\ddagger) higher.
- [38] a) The $T\Delta S$ contribution for the TS[**7–8**] + BD → TS[**7–8**]-BD process in gas-phase is calculated to amount to 11.5–12.0 kcal mol⁻¹ (298.15 K), which has to be reduced by ~6–7 kcal mol⁻¹^[26] for taking the actual catalytic reaction conditions (in liquid butadiene under pressure) into account. Thus, we estimate the entropic cost for this process to ~5 kcal mol⁻¹; b) Due to the uncertainty in the estimated entropic cost for butadiene association and dissociation processes, caused by the theoretical methodology employed in the present study, the *c,t,t*-CDT-generating path for reductive elimination certainly demonstrates a borderline case, for which we are not able to give a definite answer whether incoming butadiene is likely to participate in this process or not.
- [39] It should be noted, however, that the presence of PR₃P(OR)₃ ligands may direct the reaction almost entirely into the channel for production of C₈-cycloolefins (cf. Section F).
- [40] The overall free-energy of activation for the Ni⁰-catalyzed cyclo-trimerization of 1,3-butadiene, with all-*t*-CDT formed as the predominant product (~90% selectivity), has been estimated from available experimental data by the following crude approximation: With a TOF of 4/75 g BD per g Ni per hour at 313 K/353 K,^[9] one obtains effective rate constants $k \sim 1.21 \cdot 10^{-3}/2.26 \cdot 10^{-2} \text{ s}^{-1}$ and $\Delta G^\ddagger \sim 22.5/23.4 \text{ kcal mol}^{-1}$, respectively, by applying the Eyring equation with $k = 2.08 \times 10^{10} \text{ Texp}(-\Delta G^\ddagger/RT)$. These values agree very well with the computational estimated total barrier of ~23 kcal mol⁻¹ (ΔG^\ddagger) for the most feasible stereochemical pathway of the all-*t*-CDT generating route.

Received: July 22, 2002 [F4266]